Localization of cortical potentials evoked by balance disturbances

by

Amanda Marlin

A thesis
presented to the University of Waterloo
in fulfillment of the
thesis requirement for the degree of
Master of Science
in
Kinesiology

Waterloo, Ontario, Canada, 2011

AUTHOR'S DECLARATION

I hereby declare that I am the sole author of this thesis. This is a true copy of the thesis, including any required final revisions, as accepted by my examiners.

I understand that my thesis may be made electronically available to the public.

ABSTRACT

The ability to correct balance disturbances is essential for maintaining upright stability. Recent literature highlights a potentially important role for the cerebral cortex in controlling compensatory balance reactions. The objective of this research was to provide a more detailed understanding of the specific neurophysiologic events occurring at the cortex following balance disturbances. More specifically, the focus was to determine whether the N1, a cortical potential evoked during balance control, and the error-related negativity (ERN), a cortical potential measured in response to errors during cognitive tasks, have similar cortical representation, revealing a similar link to an error detection mechanism. It was hypothesized that the N1 and ERN would have the same generator located in the anterior cingulate cortex (ACC).

Fourteen healthy young adults participated in a balance task (evoked N1) and a flanker task (evoked ERN). Temporally unpredictable perturbations to standing balance were achieved using a lean and release cable system. Electromyography and centre of pressure were measured during the balance task. Reaction times and error rates were measured during the flanker task. Electroencephalography was recorded during both tasks. Source localization was performed in CURRY 6 using a single fixed coherent dipole model to determine the neural generator of the N1 and ERN.

The results revealed that the locations of the N1 and ERN dipoles were different. The mean (n=9) distance between N1 and ERN dipoles was 25.46 ± 8.88 mm. The mean Talairach

coordinates for the ERN dipole were (6.47 ± 3.08, -4.41 ± 13.15, 41.17 ± 11.63) mm, corresponding to the cingulate gyrus (Brodmann area 24). This represents the ACC, supporting results from previous literature. The mean Talairach coordinates for the N1 dipole were (5.74 ± 3.77, -11.81 ± 10.84, 53.73 ± 7.30) mm, corresponding to the medial frontal gyrus (Brodmann area 6). This is the first work to localize the source of the N1. It is speculated that the generator of the N1 is the supplementary motor area and that it represents the generation of a contingency motor plan to shape the later phases of the compensatory balance response based on sensory feedback from the perturbation.

ACKNOWLEDGEMENTS

I would like to extend a sincere thank you to my supervisor Dr. Bill McIlroy. Bill, I have the utmost respect for you and greatly appreciate all of your guidance, support, and encouragement over the past two years. Thank you for continually having confidence in me and for helping me keep things in perspective. I would also like to thank my committee members Dr. George Mochizuki, Dr. Richard Staines, and Dr. Laura Middleton for their insight and contribution to my thesis. Thank you to all of the Neuroscience lab members who provided their assistance, support, and most importantly, their friendship. Finally, I would like to express my deepest gratitude to my family and friends for their never-ending confidence, motivation, and patience while I completed my degree.

TABLE OF CONTENTS

LIST OF FIGURES

LIST OF TABLES

INTRODUCTION

The ability to correct balance disturbances is essential for the maintenance of upright stability. In order to correct these disturbances compensatory balance reactions are required, which become a great challenge for individuals with neurological injuries. To advance future developments of therapies to improve compensatory balance control we need to continue to develop our understanding of the central nervous system (CNS) control in healthy individuals. In spite of the considerable amount of information characterizing balance responses, the information about how the CNS controls these reactions in humans remains limited.

The control of standing balance in humans requires more than just automatic reflexes and muscle strength. In order to recover balance and maintain upright stability, higher order CNS control (i.e., the cerebral cortex) is required to integrate multiple sensory systems (e.g., visual, vestibular, and proprioception) (Maurer, Mergner, Bolha, & Hlavacka, 2000; Mergner, Maurer, & Peterka, 2003). Recent literature highlights a potentially important role for the cerebral cortex in modifying the control of upright balance (Ackermann, Diener, & Dichgans, 1986; Dietz, Quintern, & Berger, 1984; Dietz, Quintern, & Berger, 1985; Dietz, Quintern, Berger, & Schenck, 1985; Dimitrov, Gavrilenko, & Gatev, 1996; Duckrow, Abu-Hasaballah, Whipple, & Wolfson, 1999; Maki & McIlroy, 2007; Quant, Adkin, Staines, Maki, & McIlroy, 2004; Quant, Adkin, Staines, & McIlroy, 2004; Staines, McIlroy, & Brooke, 2001). The evidence comes from studies that employ dual task paradigms (McIlroy et al., 1999; Norrie, Maki, Staines, & McIlroy, 2002; Quant, Adkin, Staines, Maki, et al., 2004), which have revealed a link to executive function, indicating that cognition and attention influence balance

control (Rankin, Woollacott, Shumway-Cook, & Brown, 2000; Teasdale & Simoneau, 2001). Evidence of cortical involvement also comes from studies exploring changes in balance control in the face of specific neurological injuries (e.g., stroke) (Rapport et al., 1993). This research has revealed that patients with cortical lesions have specific deficits in the control of balance reactions. Animal studies have also demonstrated evidence of cortical cell discharge linked to evoked balance reactions (Beloozerova et al., 2003; Beloozerova, Sirota, Orlovsky, & Deliagina, 2005; Deliagina, Beloozerova, Zelenin, & Orlovsky, 2008; Karayannidou et al., 2006; Matsuyama & Drew, 2000). Most recently, electrophysiological studies with humans have further demonstrated the link between the cerebral cortex and the control of compensatory balance reactions (Adkin, Quant, Maki, & McIlroy, 2006; Dietz et al., 1984; Dietz, Quintern, & Berger, 1985; Dietz, Quintern, Berger, & Schenck, 1985; Dimitrov et al., 1996; Duckrow et al., 1999; Jacobs & Horak, 2007; Mochizuki, Boe, Marlin, & McIlroy, 2010; Mochizuki, Sibley, Cheung, & McIlroy, 2009; Mochizuki, Sibley, Esposito, Camilleri, & McIlroy, 2007; Mochizuki, Sibley, Esposito, Camilleri, & McIlroy, 2008; Mochizuki, Zabukovec, Sibley, & McIlroy, 2009; Quant, Adkin, Staines, Maki, et al., 2004; Quant, Adkin, Staines, & McIlroy, 2004; Quintern, Berger, & Dietz, 1985; Staines et al., 2001). The focus of this research was to further develop the understanding of the cortical contributors to compensatory balance control in humans.

The cortical activity related to balance tasks has been measured using positron emission tomography (PET) (Ouchi, Okada, Yoshikawa, Nobezawa, & Futatsubashi, 1999), functional magnetic resonance imaging (fMRI) (Slobounov, Wu, & Hallett, 2006), and electroencephalography (EEG). PET and fMRI provide limited opportunity to explore the

control of compensatory balance reactions. Since EEG has high temporal precision, it has the most potential to reveal cortical events that are time-locked to postural disturbances. To date, event-related potential (ERP) studies using EEG have revealed two main cortical-evoked potentials in response to applied disturbances to balance (e.g., external perturbations). There is an initial small positivity, the P1 response, representing the earliest non-specific response to instability (Dietz et al., 1984), followed by a more significant and consistently evoked negativity (N1 response). The peak of the N1 occurs approximately 100-150 ms after the onset of a perturbation in the fronto-central region of the brain (Dietz et al., 1984; Dietz, Quintern, & Berger, 1985; Dietz, Quintern, Berger, & Schenck, 1985; Dimitrov et al., 1996; Duckrow et al., 1999; Quant, Adkin, Staines, Maki, et al., 2004; Quant, Adkin, Staines, & McIlroy, 2004; Staines et al., 2001). The N1 is a large amplitude potential, ranging from 10-60 μV. The amplitude of the N1 varies since it is scaled to the amplitude of the perturbation. The amplitude of the N1 appears to be importantly influenced by the size of the perturbation (Staines et al., 2001), the predictability of the timing of the perturbation (Adkin et al., 2006; Jacobs & Horak, 2007; Mochizuki et al., 2007), a concurrent cognitive task (Quant, Adkin, Staines, Maki, et al., 2004), and a concurrent peripheral stimulus (Staines et al., 2001).

The N1 has been associated with compensatory reactions that occur following perturbations in various postures including in sitting (Mochizuki, Sibley, Cheung, Camilleri, & McIlroy, 2009; Mochizuki, Zabukovec, et al., 2009; Staines et al., 2001), standing (Adkin et al., 2006; Dietz et al., 1984; Dietz, Quintern, & Berger, 1985; Dietz, Quintern, Berger, & Schenck, 1985; Mochizuki et al., 2008, 2010; Mochizuki, Sibley, Cheung, & McIlroy, 2009; Quant, Adkin, Staines, Maki, et al., 2004), and walking (Dietz et al., 1984; Dietz, Quintern, &

Berger, 1985; Quintern et al., 1985). The N1 is also comparable across different types of tasks including inverted pendulum tilts beneath the ankle during sitting (Quant, Adkin, Staines, & McIlroy, 2004), whole-body chair tilts (Mochizuki, Sibley, Cheung, Camilleri, et al., 2009; Mochizuki, Zabukovec, et al., 2009), platform translations in sitting (Staines et al., 2001), standing (Dietz et al., 1984; Dietz, Quintern, & Berger, 1985; Dietz, Quintern, Berger, & Schenck, 1985; Quant, Adkin, Staines, Maki, et al., 2004), and walking (Dietz, Quintern, & Berger, 1985), horizontal perturbations to the trunk in standing (Adkin et al., 2006), standing lean and release (Mochizuki et al., 2008, 2010; Mochizuki, Sibley, Cheung, & McIlroy, 2009), as well as compensatory finger grips (Mochizuki, Zabukovec, et al., 2009). The specific purpose of this research was to characterize the N1 during compensatory balance reactions that were evoked by an external perturbation to upright stance (i.e., lean and release model).

There remains debate about the potential role of the N1, specifically whether it is linked to generic events such as reallocation of attentional resources or whether it is linked to the planning and execution of ongoing motor responses. Quant, Adkin, Staines, and McIlroy (2004) suggested that the N1 was not linked to the execution and planning of motor responses in their ankle pendulum study. They compared the N1 responses when participants were asked to either react or not react to perturbations (active versus passive), and discovered that a large amplitude time-locked N1 was evoked even when compensatory balance reactions were absent. It has also been suggested that the N1 represents sensory processing of the perturbation (Dietz et al., 1984; Quant, Adkin, Staines, & McIlroy, 2004). However, Mochizuki and colleagues (2008) demonstrated that the amplitude of the N1 is strongly influenced by the temporal predictability of the perturbation, independent of the evoked sensory discharge linked

to the perturbation. When the perturbation magnitude was held constant, the ability to predict the onset timing of the perturbation attenuated the N1 amplitude (Mochizuki et al., 2008). Therefore, rather than a motor or sensory linked response, we are lead to the view that the N1 is more likely an 'error' signal, reflecting a comparison between the anticipated central state and the actual state as a result of the balance disturbance (i.e., 'error' in stability) (Adkin et al., 2006; Dimitrov et al., 1996). The error detection role, suggesting a relationship between the evoked negativity and 'errors' in stability, draws parallels to a negativity evoked in other behavioural paradigms, the error-related negativity (ERN) (Pailing & Segalowitz, 2004; Yasuda, Sato, Miyawaki, Kumano, & Kuboki, 2004).

The ERN is a cortical-evoked potential that is time-locked to the execution of an erroneous response in a cognitive task. Like the N1, the ERN is a sharp negative deflection with similar amplitude, timing, and topographic representation. The ERN peaks at an amplitude of approximately 10 μV in the fronto-central region of the brain (i.e., FCz electrode location) 50-150 ms after the execution of an erroneous response in a cognitive task (Falkenstein, Hohnsbein, Hoormann, & Blanke, 1990; Gehring, Coles, Meyer, & Donchin, 1990; Gehring, Goss, Coles, Meyer, & Donchin, 1993; Gemba, Sasaki, & Brooks, 1986; Miltner et al., 2003; Sasaki & Gemba, 1986). Also in accordance with the N1, the ERN is comparable across a variety of different tasks. The ERN occurs in tasks involving decision making when executed errors are easy to detect (Fiehler, Ullsperger, & von Cramon, 2005), including choice reaction time tasks (Gehring et al., 1993), go/no-go response inhibition tasks in humans (Falkestein, Koshlykova, Kiroj, Hoormann, & Hohnsbein, 1995; Gemba & Sasaki, 1989; Kiefer, Marzinzik, Weisbrod, Scherg, & Spitzer, 1998; Kiehl, Liddle, & Hopfinger,

2000; Menon, Adleman, White, Glover, & Reiss, 2001; Miltner et al., 2003; Roberts, Rau, Lutzenberger, & Birbaumer, 1994; Scheffers, Coles, Bernstein, Gehring, & Donchin, 1996) and monkeys (Gemba et al., 1986; Sasaki & Gemba, 1986), letter and tone discrimination tasks (Pailing & Segalowitz, 2004), and various versions of the flanker task (Falkenstein, Hoormann, Christ, & Hohnsbein, 2000; Fiehler et al., 2005; Scheffers & Coles, 2000; Ullsperger & von Cramon, 2001).

Similar to the N1, there remains debate about the role of the ERN. It has been suggested that the ERN is linked to a reinforcement learning process where the basal ganglia monitors behaviour and the anterior cingulate cortex (ACC) decides which competing mental process gains access to the motor system (Holroyd & Coles, 2002). When the behaviour is worse than expected, the basal ganglia signals the ACC of the error by decreasing its dopaminergic innervation, transiently preventing its inhibitory influence on the ACC, resulting in the ERN (Holroyd & Coles, 2002). Another theory related to competing processes suggests that the ERN represents a response conflict monitor (Carter et al., 1998; Miltner, Braun, & Coles, 1997; van Veen & Carter, 2002a,b; Yeung et al., 2004). As a response conflict monitor, the ACC detects, during error trials, that incompatible processes are active at the same time (i.e., conflicting activation of the rapid erroneous response and slightly slower correct response, which emerges due to ongoing evaluation of the stimulus) (van Veen & Carter, 2002a,b). However, Ullsperger and von Cramon (2001) demonstrated that monitoring response conflict and detecting errors are two different systems since cortical activation during error trials was different than the activation during correct trials with high response conflict. The pre-supplementary motor area (pre-SMA) was activated during correct trials with high

response conflict, suggesting that it has a role in overcoming obstacles between the planning and execution of a motor action before the action actually occurs (Ullsperger & von Cramon, 2001). In contrast, the ACC was activated during error trials, suggesting that it has a role in detecting errors after they have occurred (Ullsperger & von Cramon, 2001). Since the ERN is only seen in error trials, it is speculated that it is related to a general error detection mechanism that monitors and compares a representation of the intended correct response to a representation of the actual response (Bernstein, Scheffers, & Coles, 1995; Coles, Scheffers, & Holroyd, 1998, 2000; Dehaene, Posner, & Tucker, 1994; Falkenstein et al., 2000; Gehring et al., 1993; Miltner et al., 2003; Scheffers & Coles, 2000; Ullsperger & von Cramon, 2001).

A better understanding of the location of the generators of the activity related to both the N1 and the ERN may help guide an understanding about their possible role. Based on the topographic representation (i.e., fronto-central region of the brain), the possible candidates for the origin of both responses are the SMA or deeper structures such as the ACC. To date, no studies have localized the cortical area where the N1 occurs; however, preliminary current density reconstruction by Mochizuki, Zabukovec, and colleagues (2009) demonstrated cortical activation concentrated in the central region of the brain following chair tilts and compensatory finger grips. On the other hand, much research has focused on the localization of the ERN. Brain electrical activity source analysis has suggested a medial frontal generator (Coles et al., 1998; Dehaene et al., 1994; Falkenstein, Hohnsbein, Hoormann, & Blanke, 1991; Holroyd, Dien, & Coles, 1998; Miltner, Lemke, Holroyd, Scheffers, & Coles, 1998), possibly originating in the ACC and/or medial frontal gyrus (e.g., SMA) (Gehring, 1992). However, as stated previously, Ullsperger and von Cramon (2001) demonstrated that the SMA might be

involved in a different system for monitoring response conflict since the activation is different in error trials than those in correct trials with high response conflict. The role of this system may be to overcome obstacles between the planning and execution of a motor action before the action actually occurs. Whereas, the ACC (in particular, cingulate motor area, which has dense connections with the primary motor cortex and spinal cord) has been associated with detecting an error once it has already occurred, potentially using the information to correct the behaviour (Ullsperger & von Cramon, 2001). The ACC has been implicated in error processing by neurophysiological studies in monkeys (e.g., Gemba et al., 1986; Niki & Watanabe, 1979; Shima & Tanji, 1998), fMRI studies in humans (e.g., Carter et al., 1998; Carter, MacDonald, Ross, & Stenger, 2001; Holroyd et al., 2004; Kerns et al., 2004; Kiehl et al., 2000; Menon et al., 2001; Ullsperger & von Cramon, 2003), as well as dipole source localization studies in humans (e.g., Badgaiyan & Posner, 1998; Dehaene et al., 1994; Holroyd et al., 1998; Miltner et al., 1997, 2003). Thus, if the N1 is also an error detector, it may have the same generator as the ERN (i.e., ACC).

Objectives & Hypotheses

The overall objective of this research was to provide a more detailed understanding of the specific neurophysiologic events that occur at the cortex following a balance disturbance and their link to the control of upright stability. More specifically, the focus of this study was to determine whether the N1, evoked during balance control, and the ERN, measured in response to errors during cognitive tasks, have similar cortical representation, potentially revealing a similar link to an error detection mechanism. In order to probe the underlying processes and infer similarities between the negativities we assessed EEG characteristics and localized the

generator of each response using dipole source localization. Based on the suggestion that the N1 may be related to error detection (Adkin et al., 2006) and the fact that the ACC is associated with error processing during cognitive tasks (van Veen & Carter, 2002a,b), it was hypothesized that the N1 and the ERN would have the same generator and that this common generator would be located in the ACC. Similar source location, combined with similar EEG characteristics (i.e., timing and topographic representation) would reinforce the view that the N1 and ERN have the same circuitry and function, and therefore, potentially represent the same error detection mechanism. Such understanding would continue to advance our knowledge of the underlying CNS control of compensatory balance.

METHODOLOGY

Participants

Fourteen healthy young adults provided informed consent to participate in this study. Participants were asked to complete a brief questionnaire about their medical history indicating that they were free of neurological and musculoskeletal conditions that could have impacted task performance. This study received ethics clearance through the Office of Research Ethics at the University of Waterloo.

Experimental Protocol

Each participant performed two tasks, a lean and release task in order to evoke the N1 and a flanker task in order to evoke the ERN. The task order was counter-balanced across participants.

Lean & Release Task

Perturbations to standing balance were achieved using a custom lean and release cable system (figure 1) that reliably evoked compensatory balance reactions. The participant stood on a force plate in a standard foot position with their heel centres 17 cm apart and a 14° angle between the long axes of the feet (McIlroy & Maki, 1997). This was marked on the force plate with black electrical tape in order to ensure consistency between trials and between individuals. The participant stood with a slight forward lean in order to create tension in the cable that was affixed to their harness from behind. The participant was asked to focus on a fixation point that was marked with black electrical tape on the wall in front of them in order to

reduce eye movements since they create artifact in the EEG signal. The experimenter applied the perturbation by releasing the tension in the cable (releasing a seatbelt buckle), causing the participant to fall in a forward direction, evoking a compensatory reaction. The magnitude of the perturbation was only large enough (5-7% of the participant's body weight) to evoke a feet-in-place reaction (e.g., ankle or hip strategy) to recover balance. The timing of each perturbation was randomized and varied from 1 to 15 seconds once the participant was relaxed in the forward lean position. The perturbations were temporally unpredictable to the participant. A total of 40 trials were collected for each participant. Electroencephalography, electromyography (EMG), and centre of pressure (COP) were recorded prior to, during, and following the application of perturbations to upright stance.

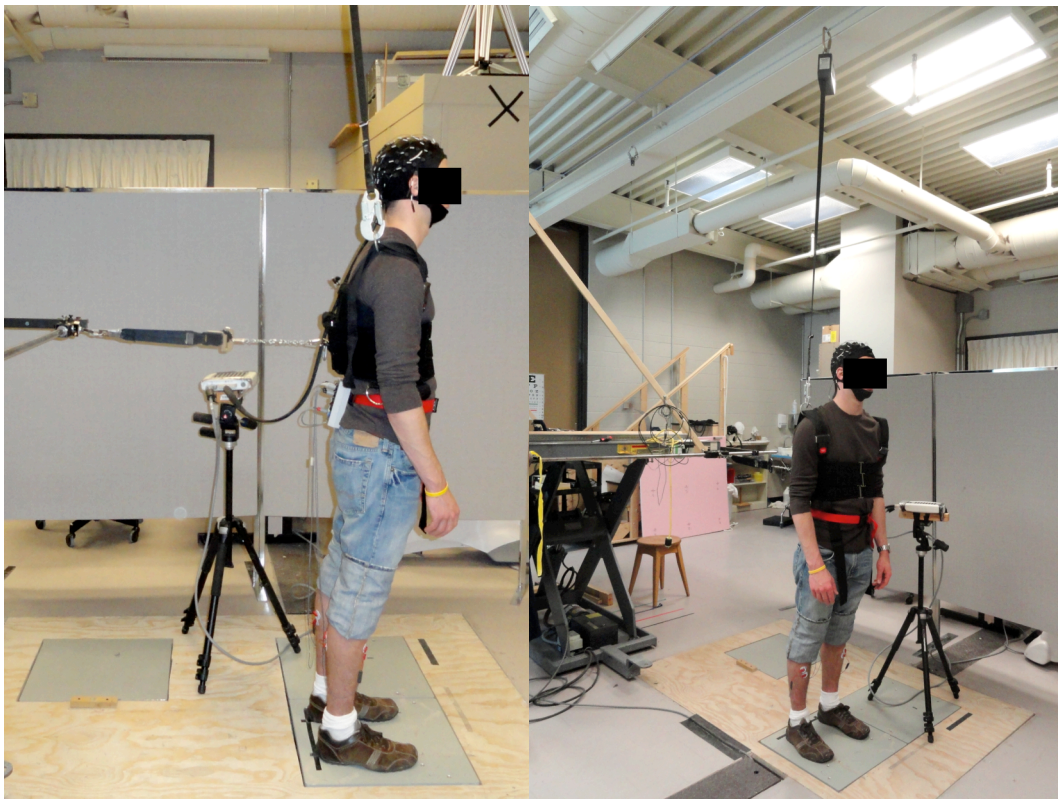

Figure 1. Lean and release cable system that reliably evoked compensatory balance reactions.

Flanker Task

The participants also performed a speeded modified flanker task (figure 2) in order to evoke the ERN. The flanker task utilized in the present study was based on the parameters used by Ullsperger and von Cramon (2001), which produces high error rates (Kopp, Rist, Mattler, 1996 in Ullsperger & von Cramon, 2001). The participants were instructed to respond as fast and as accurately as possible to the direction of a target arrow that was presented briefly on the centre of a computer screen with either a left or right mouse button press. All responses were performed with the right hand. The trial began with the participant looking at a fixation mark for 500 ms. Immediately following the 500 ms fixation period, four flanker arrows of irrelevant direction were displayed on the screen for 80 ms. The target arrow then appeared on the screen for 30 ms and was positioned in the centre of the four flanker arrows (replacing the fixation mark). Immediately following the 30 ms display of the target arrow, all arrows were removed from the screen and the fixation mark was displayed for 450 ms. During this time period the participant responded to the direction of the target arrow as fast and as accurately as possible by clicking the right mouse button if the target arrow was pointing to the right or the left mouse button if the target arrow was pointing to the left. Following the response period, there was a 900 ms window that either displayed the fixation mark or "Respond faster!" if the participant did not respond within the 450 ms window. This sequence was repeated for 10 minutes, during which approximately 300 responses were required. Fifty percent of the trials were congruent (i.e., flanker arrows and target arrow were pointing in the same direction) and the other 50% were incongruent (i.e., flanker arrows and target arrow were pointing in opposite directions). The congruent and incongruent trials were randomized over the 10-minute block. Each participant performed five 10-minute blocks in order to achieve an adequate number of error

trials for ERP analysis. The participants were given a 1 to 2 minute break between blocks in order to prevent fatigue and loss of concentration.

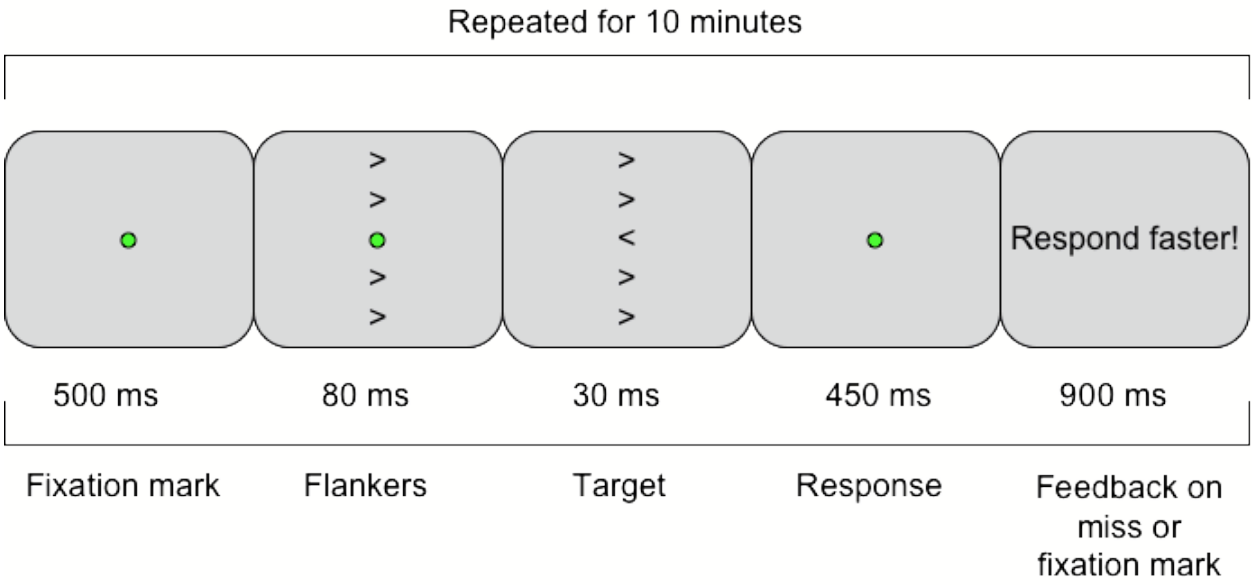

Figure 2. Timeline for the flanker task. The stimulus displayed represents an incongruent trial.

Data Acquisition

Electroencephalography

To quantify cortical activity during lean and release trials as well as the flanker task, evoked potentials were recorded using a 64-channel electrode cap (Neuroscan, El Paso, TX), based on the 10-20 system of electrode placement. All channels were referenced to linked mastoids and the impedance was less than 5 kΩ. Electrooculography (EOG) signals were recorded using four Ag/AgCl electrodes (7 mm diameter). The electrodes were positioned superior and inferior to the left eye as well as lateral to the left and right eyes. The skin was abraded (Nuprep ECG & EEG Abrasive Skin Prepping Gel, Weaver & Company, Aurora, CO) and

cleaned with rubbing alcohol prior to electrode placement. All EEG and EOG electrodes were filled with isoelectric gel (Electro-Gel, Electro-Cap International, Inc., Eaton, OH). All EEG and EOG signals were filtered (DC-300 Hz) online using a SynAmps2 amplifier (Neuroscan, El Paso, TX) and were sampled at a rate of 1000 Hz. The data was stored for offline analysis.

Additionally, during the flanker task, the LabVIEW program (National Instruments, Austin, TX) that controlled the visual stimuli marked the Neuroscan continuous file with square wave pulses upon presentation of each target arrow. The program also marked the Neuroscan continuous file with a square wave pulse each time the participant responded to the target arrow with a button press indicating the timing of the onset of the response, whether the response was correct (positive voltage) or incorrect (negative voltage), and whether it was a congruent or incongruent trial. Following the collection of the first six participants, a second version of the flanker task was created in Stim^2 (Neuroscan, El Paso, TX), and was used for the eight remaining participants. The Stim^2 system also marked the stimuli and button presses on the Neuroscan continuous file. This information was used during post-processing to separate the trials into congruent and incongruent as well as to determine reaction times and error rates.

Electrode Position

The Polhemus Tracking System (3DSpaceDX, Neuroscan, El Paso, TX) was used to digitize the precise position of the 64 electrode sites on each participant's head, creating a three-dimensional (3D) image. The coordinates of the participant's left and right preauricular points and nasion were used as the reference plane for all 64 electrode positions. During post-processing these 3D coordinates (X, Y, and Z in mm) were imported into CURRY 6

(Compumedics Neuroscan, Charlotte, NC) and co-registered with the participant's structural MRI (sMRI) for source localization.

Image Acquisition

Structural MRIs were obtained for all participants at one of five locations: Sunnybrook Health Sciences Centre (Toronto, ON), Toronto Western Hospital (Toronto, ON), Baycrest Centre for Geriatric Care (Toronto, ON), Grand River Hospital (Kitchener, ON) and University of Alberta Hospital (Edmonton, AB). At all sites, a standard 3D high-resolution T1-weighted image was collected on a research scanner. The details of the scan parameters (which were unique to each site and required for CURRY analysis) are provided in table 1.

Table 1. sMRI parameters for five locations.

Location	Sunnybrook	Toronto Western	Baycrest	Grand River	University of Alberta
Scanner type	3 Tesla, GE Medical Systems, Discovery MR750	3 Tesla, GE Medical Systems, Signa HDx	3 Tesla, Siemens, Trim Trio	1.5 Tesla, Philips Medical Systems, Intera	1.5 Tesla, Siemens, Sonata
# Pixels (X)	256	256	192	240	384
# Pixels (Y)	256	256	256	240	512
Pixel spacing	0.8594 \ 0.8594	0.9375 \ 0.9375	1.0 \ 1.0	1.0 \ 1.0	0.5 \ 0.5
# Slices	152	172	160	150	176
Slice thickness (mm)	1.0	1.1	1.0	1.0	1.0
Spacing between slices (mm)	0.0	0.0	0.0	0.0	0.0
Slice orientation	Axial	Axial	Axial	Axial	Axial
Bits allocated	16	16	16	16	16
Byte order	Little Endian	Little Endian	Little Endian	Little Endian	Little Endian

Electromyography

To capture and characterize the onset of the compensatory balance reaction, EMG was recorded from medial gastrocnemius (MG) and tibialis anterior (TA), bilaterally. EMG was also recorded from bilateral upper trapezius (UT) in order to capture neck muscle activity and screen for possible artifact on EEG tracings. Two surface Ag/AgCl electrodes (Kendall Medi-Trace 130 ECG Conductive Adhesive Electrodes, Tyco Healthcare Group LP, Mansfield, MA) were oriented approximately 2 cm apart longitudinally over the predicted fibre paths of each muscle. The skin was abraded (Nuprep ECG & EEG Abrasive Skin Prepping Gel, Weaver & Company, Aurora, CO) and cleaned with rubbing alcohol prior to electrode placement. Impedance was less than 5 kΩ, measured at 30 Hz (Grass EZM5 Electrode Impedance Meter, Grass Instrument Co., Quincy, MA). The signal was amplified 1000x with an isolated bioelectric amplifier (AMT-8, Bortec Biomedical Inc., Calgary, AB) and digitized at an analog-digital interface (BNC-2111, National Instruments Corporation, Austin, TX) with a sampling rate of 1000 Hz. The data was collected over a 15-second window, within which the perturbation randomly occurred, and was stored for offline analysis.

Centre of Pressure

The position of the anterior-posterior (AP) COP was recorded in order to characterize the compensatory balance reactions by having the participants stand with both feet on the same force plate (50.5 cm wide, 46 cm long; Advanced Medical Technology Inc., Watertown, MA). The COP signal was digitized at an analog-digital interface (BNC-2111, National Instruments Corporation, Austin, TX) with a sampling rate of 1000 Hz. The data was collected over a 15-

second window, within which the perturbation randomly occurred, and was stored for offline analysis.

Lean Force

Prior to the perturbation the participant was secured to an electric powered lift platform with a cable. One end of the cable was connected to the back of the participant's safety harness and the other end was connected to an in-line load cell (Transducer Techniques, Temecula, CA) that was affixed to the lift. The force on the load cell indicated the amount of force the participant was exerting on the cable, allowing for the quantification of the lean angle prior to the perturbation. The participant's lean angle was adjusted, using a different number of chain links to make the cable shorter or longer, until the force on the cable was 5-7% of the participant's body weight, ensuring consistent perturbation magnitude between participants. The lean force was monitored at the beginning of every trial to ensure that it remained consistent throughout the duration of the collection. The force on the load cell was digitized at an analog-digital interface (BNC-2111, National Instruments Corporation, Austin, TX) with a sampling rate of 1000 Hz. The data was collected over a 15-second window, within which the perturbation randomly occurred, and was stored for offline analysis. This data was also sent via a high level input to mark the Neuroscan continuous file, indicating the onset of the perturbation (i.e., time point at which there was a sharp decrease in force on the cable).

Data Analysis

Electroencephalography

Post-processing for the EEG data was done in Neuroscan 4.3 (El Paso, TX). The same analysis steps were utilized for both task conditions. Epochs were response-locked to the onset of the perturbation or button press, which were marked as events, via a numeric trigger, on the EEG continuous recording. The duration of each epoch was from 600 ms before the onset of the event to 500 ms after the onset of the event (i.e., -600 ms to 500 ms). Each epoch was low-pass filtered at 30 Hz and baseline corrected using the average amplitude of the first 100 ms of that epoch (i.e., -600 ms to -500 ms). Each epoch was then visually scanned for ocular artifact and epochs with blinks or horizontal eye movements were rejected from all analyses. For participants with an excessive number of blinks, the Ocular Artifact Reduction transformation was utilized in Neuroscan in order to avoid having to exclude an unacceptable number of epochs. This transformation averages the artifact in an EOG channel and subtracts it from the EEG channels. Following the removal or reduction of ocular artifact, the remaining epochs were averaged on the onset of the event within participants and then across participants.

To characterize the N1 and ERN, the latency and amplitude of post-perturbation and post-error cortical potentials were measured for each individual participant. Data was averaged across trials for each individual with respect to the onset of the perturbation for lean and release trials and the onset of the error for the flanker task (time 0). From each individual's averaged response, N1 and ERN latencies were determined by marking the time of the negative peak that occurred within 500 ms of the perturbation and error onset (time 0), respectively. The amplitude of the N1 was recorded as the absolute amplitude at the negative

peak. The amplitude of the ERN was determined by calculating the difference in voltage between that at the peak of the positivity preceding the negativity (i.e., onset of the negativity) and that at the peak of the negativity. The mean amplitudes and latencies of the N1 and ERN were calculated across all participants. Analysis of the amplitude and timing of both negativities was limited to the electrode site where the amplitude of the negativity was maximal (i.e., FCz).

In order to further reduce noise in the EEG waveforms, each participant's averaged N1 and ERN waveforms were filtered using independent component analysis (ICA) in Neuroscan. The ICA time interval was set using the electrode site where the amplitude of the peak negativity was maximal (i.e., FCz). The time interval began at the positive peak immediately prior to the negative peak following the onset of the perturbation for lean and release trials or the onset of the error for the flanker task. The time interval ended at the positive peak immediately following the negative peak. In order to determine the number of valid components for the ICA, principle component analysis (PCA) was utilized. PCA components that explained greater than 4.0% of the overall variance were considered valid. PCA components that explained less than 4.0% of the overall variance were excluded as they were assumed to represent noise. The ICA components were then calculated based on the subspace selected in the PCA. Determining the inclusion of ICA components was based on the degree to which the component appeared as the N1 or ERN waveform (i.e., peaks occurring in phase), the topographic distribution (i.e., negative in the fronto-central region of the brain), as well as how it contributed to the overall mean global field power (MGFP). The MGFP is a collapsed average and measure of signal strength (i.e., signal-to-noise ratio; SNR) of all EEG channels

(Compumedics Neuroscan, 2007). The resulting ICA filtered EEG data was utilized for source localization.

Source Localization

Localization of the N1 and ERN was conducted during post-processing in CURRY, separately for each task condition for each participant. Source localization relied on a full cap EEG recording, precise electrode positions (Polhemus Tracking System), and a realistic model of the head (sMRI).

The first step in source localization involved importing each participant's averaged and ICA filtered EEG data into CURRY, separately for each task condition. Noise estimation was performed on the EEG data by calculating the variance of a user defined time interval for all channels. The MGFP was utilized to determine the 100 ms pre-stimulus window with the lowest signal content, which presumably contained only noise. For all participants the noise estimation was performed in an interval that had an average noise level of < 1 μV and a maximum SNR of > 10 μV. The estimated noise level was compared to the residual error during dipole analysis in order to determine the plausibility of the localization.

The second step in source localization was to create a 3D model of the cerebral cortex via a region growing segmentation algorithm beginning at the seed point of each participant's sMRI (i.e., centre of the image). The segmentation result was based on segmentation thresholds for different tissue types that were defined for each participant's sMRI. Starting at the seed point, the volume (i.e., 3D model) grew outward until the threshold for the cortex was

violated. Additionally, a realistic model of the head, or high resolution boundary element model (BEM), was constructed via triangulation (5000 nodes, 10000 triangles) of three compartments: the skin, outer skull, and inner skull/brain, with thicknesses of 9.0 mm, 8.0 mm, and 6.0 mm, and fixed conductivities of 0.33, 0.0042, and 0.33 S/m, respectively. The BEM model was based on the defined segmentation thresholds and seed slice from the sMRI.

The third step involved the co-registration of each participant's sMRI and the 3D coordinates of each electrode position. Co-registration involved identifying the nasion and left and right pre-auricular points on each participant's sMRI and matching these with the 3D coordinates of the same three landmarks that were recorded with the Polhemus Tracking System during data collection. The electrode positions were then aligned to the 10-20 system based on the skin segmented from the sMRI in order to correspond with the electrode placement during collection.

The fourth step involved defining the Talairach system by manually marking various points on each individual's sMRI. The anterior commissure (AC) was marked as the origin of the Talairach system, the posterior commissure (PC) was marked as the point at which the negative Y axis passed through, and a mid-sagittal point in the inter-hemispheric fissure was marked as the point through which the Talairach (y, z) plane passed. Additionally, in order to transform the sMRI into Talairach space, the borders of the brain with respect to the AC (i.e., anterior, superior, inferior, left, and right borders) and PC (i.e., posterior border) were manually marked. Thus, the Talairach coordinates reported from the dipole analysis were scaled to match the Talairach atlas based on the marked boundaries of the brain.

Finally, dipole analysis was performed in order to compute a local source model that solved the inverse problem (i.e., unknown source of EEG signal) and represented the brain activity at the peak of the N1 and ERN. One dipole was located using the fixed coherent model since the location and orientation of the dipole were assumed fixed over time. Thus, for all time points, common positions and orientations were fitted (Compumedics Neuroscan, 2007). The dipole analysis was performed on a 20 ms time interval surrounding the peak negativity of the MGFP for each task condition. For lean and release trials, the time interval began 10 ms prior to the peak negativity that occurred within 500 ms of the onset of the perturbation, representing the N1. For the flanker task, the time interval began 10 ms prior to the peak negativity that occurred within 500 ms of the onset of the button press (i.e., error), representing the ERN. For each task condition the time interval ended 10 ms following the peak negativity. The location of each dipole was reported in Talairach coordinates, (x, y, z) mm. The orientation of each dipole was also reported (nx, ny, nz). The Talairach coordinates were used, by representing them as position vectors with respect to an origin, to calculate the distance between the N1 and ERN dipoles for each participant with the formula below. The mean distance between dipoles was then calculated across participants.

$$\text{Distance (mm)} = \sqrt{[(x_2 - x_1)^2 + (y_2 - y_1)^2 + (z_2 - z_1)^2]}$$

The locations of the N1 and ERN dipoles were considered different if the distance between them was greater than the average EEG source localization error of 10.5 ± 5.4 mm, determined by Cuffin, Schomer, Ives, and Blume (2001) using a realistic head shape model (BEM) and implanted depth electrodes.

Perturbation Onset & Lean Force

The perturbation onset for each trial was determined in a custom LabVIEW program. The cable force data was first filtered with a fourth order low pass Butterworth filter (75 Hz). The mean amplitude (V) and 99% confidence band was determined for a 500 ms time window that began 750 ms prior onset of the perturbation. The point at which the cable force dropped to 0 V was then detected. The program then looked backward from the 0 V point until the cable force entered the confidence band of the pre-perturbation interval. This point was marked as the onset of the perturbation. This information was used to calculate the onset of EMG and AP COP excursions with respect to the onset of the perturbation. The lean force was calculated as the mean cable load (V) of the 500 ms time window that began 750 ms prior to the onset of the perturbation. This mean value was then converted to a percentage of body weight (% BW). This was calculated for each trial and then averaged across trials for each participant. The mean lean force across all participants was then calculated.

Electromyography

EMG responses during perturbation trials were analyzed in a custom LabVIEW program. The first steps of EMG analysis involved applying a second order band pass Butterworth filter (20-250 Hz), baseline correction, and full-wave rectification. The mean amplitude (V) and 99% confidence band were determined for a 300 ms time window prior to the onset of the perturbation (-300 ms to 0 ms). The latency of the initial EMG burst following the perturbation was defined as the point at which the EMG amplitude exceeded this 99% confidence band for 25 ms or longer. In order to determine EMG onset latencies, the full-wave rectified data was used to detect the first threshold break. A second order low pass Butterworth filter (50 Hz) was

then applied to the full-wave rectified data. This filtered data was used to determine the duration of the burst. In order to be considered the EMG onset, the burst was required to remain above the threshold for at least 25 ms. The filtered data was used for detecting the duration of the burst because the high frequency data was likely to drop below the threshold sooner than 25 ms. The point at which the EMG amplitude exceeded the threshold for longer than 25 ms was marked back onto the full-wave rectified data to record the precise onset time (ms). This method is consistent with previous research (Hodges & Bui, 1996). The EMG onset was determined and marked automatically, however, each trial was visually scanned for accuracy and repositioned if necessary. In order to quantify the magnitude of the EMG response, total integrated EMG (mVms) was calculated over the first 75 ms, 100 ms, and 200 ms after EMG onset ($iEMG_{75}$, $iEMG_{100}$, and $iEMG_{200}$). This analysis was done separately for each muscle (i.e., bilateral MG, bilateral TA, and bilateral UT) for each participant.

In order to screen for EMG responses prior to the onset of the perturbation as a result of anticipating the event, the onset latencies as well as the mean pre-perturbation amplitudes (i.e., the mean of the 300 ms window before the onset of the perturbation) for left and right MG muscles were statistically analyzed using the univariate procedure. The stem leaf, box plot, normal probability plot, and histogram were examined for each onset latency and pre-perturbation amplitude for each trial in order to distinguish outliers. Trials that appeared as outliers for onset latency were rejected from all analyses based on the criteria of an EMG response occurring earlier than 50 ms following the onset of the perturbation. Late EMG responses (i.e., onset latencies greater than 300 ms following the onset of the perturbation) were also removed from all analyses. These criteria are consistent with previous literature (e.g.,

Adkin et al., 2006). Trials that appeared as outliers for pre-perturbation amplitude were visually scanned in a custom LabVIEW program in order to determine whether the amount activity prior to the perturbation was small or large with respect to the post-perturbation EMG burst. If the SNR was low (i.e., a large amount of activity pre-perturbation with respect to post-perturbation activity), the trial was removed from all analyses. The trials were also visually scanned to determine if the pre-perturbation activity was tonic or phasic. If the activity was phasic the trials were rejected from all analyses based on the assumption that this indicated anticipatory activity in preparation for the perturbation (i.e., increasing EMG activity leading up to the perturbation). Trials with a large amount of UT EMG activity following the onset of the perturbation were excluded from all analyses to avoid related noise in the EEG data.

Centre of Pressure

Anterior-posterior COP excursions were analyzed in a custom LabVIEW program. The AP COP data was first filtered with a fourth order low pass Butterworth filter (15 Hz). In order to determine the onset of the AP COP excursion, the mean (cm) and standard deviation for a baseline pre-perturbation interval (first 1000 ms of the trial) were established for each trial. The AP COP onset was defined as the point at which the amplitude exceeded five standard deviations of the baseline mean value (Mochizuki et al., 2008) and was reported as the time to AP COP onset (ms) after the onset of the perturbation. The peak of the AP COP excursion (within 500 ms of the AP COP onset) was detected automatically using a peak detection function in LabVIEW. The amplitude of the AP COP (cm) response was calculated as the difference between the peak value and the mean baseline value. The time to the AP COP peak (ms) was reported with respect to the onset of the perturbation.

Reaction Times & Error Rates

The reaction times and error rates during the LabVIEW flanker task were calculated in a custom LabVIEW program using the square wave pulses stored during the task. The square waves indicated the timing of the stimulus onset as well as the timing of the participant's button press, allowing the calculation of reaction time. The square waves also indicated whether the response was correct (positive voltage) or incorrect (negative voltage), allowing the calculation of error rate. The different voltages of the square waves indicated whether each trial was congruent or incongruent, allowing comparison between trial types. The reaction times for the Stim^2 flanker task were calculated within Stim^2 during data collection and saved in a text file at the end of each block. This text file also contained information about whether the participant responded correctly or incorrectly for each trial and whether each trail was congruent or incongruent, similarly allowing for the calculation of error rate and the comparison between trial types.

RESULTS

Participants

Fourteen participants (nine females and five males), with an average age of 26.57 ± 4.43 years, participated in this study. Three participants were excluded from all analyses due to excessive artifact in their EEG data that masked the N1 and/or ERN. One participant was removed from source localization due to challenges in segmenting the cerebral cortex from their sMRI, rendering dipole analysis inaccurate. A final participant was removed from the mean Talairach coordinates for each dipole since their ERN dipole was located superior to the cerebral cortex, likely due to the fact that the participant had a very small number of error trials.

Behavioural Data

For the lean and release task, the mean percentage body weight for the cable force across all trials for 11 participants was 5.50 ± 0.89%. Compensatory balance reactions were present in all trials, demonstrated by rapid MG activation and AP COP excursions following the balance disturbances. Figure 3 shows the typical EMG and COP responses for one participant following a balance perturbation. Tables 2-4 report MG and TA EMG onset latencies, MG EMG amplitudes, and TA EMG amplitudes, respectively, following perturbations for 11 participants. Table 5 reports AP COP onset latencies and peak latencies as well as peak amplitudes following perturbations for 11 participants. Finally, table 6 reports reaction times and error rates for the flanker task for 11 participants.

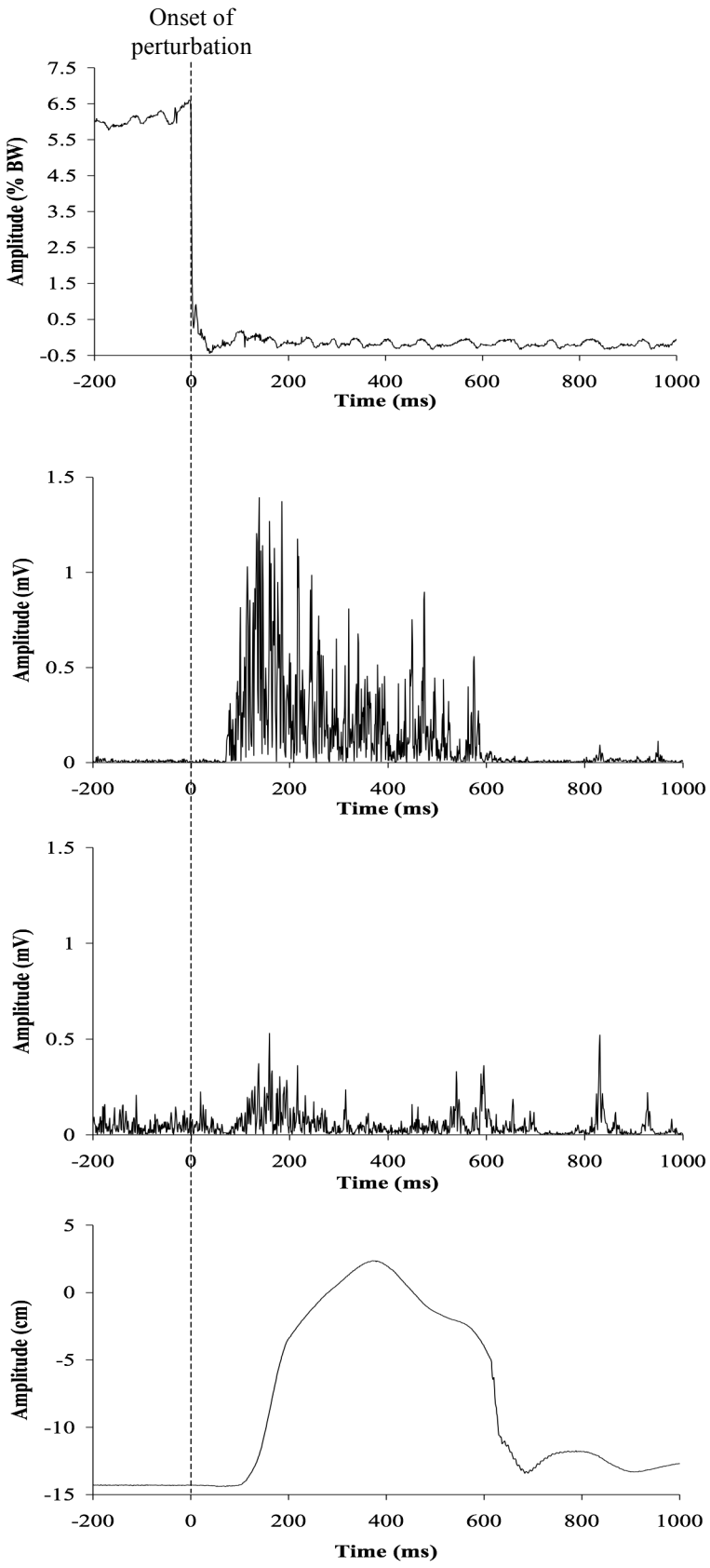

Figure 3. Lean force (panel 1), right MG EMG (panel 2), right TA EMG (panel 3), and AP COP excursion (panel 4) during a lean and release trial for participant 13 (raw data). Time 0 represents the onset of the perturbation.

Table 2. EMG onset latencies following balance perturbations for 11 participants. The perturbations occurred at time = 0 ms. Values are presented as mean ± standard deviation.

ID #	EMG onset latency (ms)			
	Left MG	**Right MG**	**Left TA**	**Right TA**
02	174.80 ± 8.93	180.44 ± 8.13	203.73 ± 32.22	203.96 ± 31.20
03	171.90 ± 10.85	179.78 ± 10.97	200.33 ± 15.40	205.60 ± 10.38
04	181.75 ± 7.65	179.35 ± 8.08	185.93 ± 29.35	189.74 ± 29.97
05	167.71 ± 10.45	173.34 ± 11.02	189.73 ± 28.78	198.04 ± 18.64
06	201.71 ± 18.20	197.51 ± 16.75	212.67 ± 25.83	223.26 ± 61.34
09	186.09 ± 10.84	185.34 ± 8.27	220.32 ± 23.83	202.66 ± 11.55
10	193.74 ± 14.03	187.34 ± 13.16	207.93 ± 25.89	251.32 ± 62.67
11	186.68 ± 13.51	194.79 ± 10.53	219.99 ± 30.47	226.51 ± 49.09
12	181.63 ± 10.38	189.88 ± 10.32	169.17 ± 86.69	217.11 ± 14.74
13	189.25 ± 9.96	179.37 ± 8.35	225.29 ± 19.80	222.07 ± 25.86
14	179.09 ± 7.85	177.91 ± 7.65	186.05 ± 8.04	198.36 ± 14.39
Mean (n=11)	**182.79 ± 14.77**	**183.72 ± 12.63**	**201.77 ± 36.83**	**211.68 ± 38.01**

Table 3. MG EMG amplitudes for 11 participants integrated over the first 75 ms, 100 ms, and 200 ms following EMG onset. Values are presented as mean ± standard deviation.

ID #	Left MG amplitude (mVms)			Right MG amplitude (mVms)		
	75 ms	**100 ms**	**200 ms**	**75 ms**	**100 ms**	**200 ms**
02	0.00452 ± 0.00400	0.00589 ± 0.00442	0.00957 ± 0.00572	0.00334 ± 0.00191	0.00394 ± 0.00194	0.00604 ± 0.00263
03	0.0101 ± 0.00218	0.0135 ± 0.00267	0.0206 ± 0.00460	0.00761 ± 0.00203	0.0106 ± 0.00238	0.0182 ± 0.00314
04	0.00123 ± 0.000445	0.00138 ± 0.000460	0.00238 ± 0.000519	0.00186 ± 0.000643	0.00203 ± 0.000636	0.00348 ± 0.000662
05	0.0103 ± 0.00349	0.0153 ± 0.00395	0.0258 ± 0.00584	0.00545 ± 0.00157	0.00744 ± 0.00151	0.0119 ± 0.00248
06	0.00176 ± 0.000660	0.00259 ± 0.000834	0.00508 ± 0.00130	0.00211 ± 0.000881	0.00315 ± 0.00112	0.00688 ± 0.00135
09	0.0165 ± 0.00364	0.0240 ± 0.00601	0.0473 ± 0.00941	0.00968 ± 0.00229	0.0128 ± 0.00307	0.0210 ± 0.00402
10	0.0100 ± 0.00330	0.0126 ± 0.00476	0.0248 ± 0.00877	0.00550 ± 0.00161	0.00633 ± 0.00192	0.0128 ± 0.00414
11	0.0135 ± 0.00354	0.0203 ± 0.00433	0.0342 ± 0.00793	0.0139 ± 0.00372	0.0197 ± 0.00505	0.0388 ± 0.00804
12	0.0241 ± 0.00659	0.0329 ± 0.00770	0.0693 ± 0.0187	0.0153 ± 0.00563	0.0191 ± 0.00681	0.0305 ± 0.0106
13	0.0153 ± 0.00367	0.0215 ± 0.00453	0.0409 ± 0.00676	0.0204 ± 0.00497	0.0303 ± 0.00672	0.0645 ± 0.00963
14	0.0196 ± 0.00413	0.0228 ± 0.00414	0.0296 ± 0.00689	0.0265 ± 0.00529	0.0297 ± 0.00593	0.0368 ± 0.00824
Mean (n=11)	**0.0113 ± 0.00776**	**0.0154 ± 0.0103**	**0.0275 ± 0.0205**	**0.00972 ± 0.00820**	**0.0126 ± 0.0103**	**0.0216 ± 0.0182**

Table 4. TA EMG amplitudes for 11 participants integrated over the first 75 ms, 100 ms, and 200 ms following EMG onset. Values are presented as mean ± standard deviation.

ID #	Left TA amplitude (mVms)			Right TA amplitude (mVms)		
	75 ms	**100 ms**	**200 ms**	**75 ms**	**100 ms**	**200 ms**
02	0.00233 ± 0.00243	0.00308 ± 0.00245	0.00608 ± 0.00252	0.000943 ± 0.00134	0.00120 ± 0.00135	0.00249 ± 0.00138
03	0.00181 ± 0.000680	0.00250 ± 0.000870	0.00541 ± 0.00156	0.00127 ± 0.000373	0.00178 ± 0.000462	0.00359 ± 0.000706
04	0.000667 ± 0.000239	0.000785 ± 0.000302	0.00126 ± 0.000342	0.000462 ± 0.000175	0.000549 ± 0.000191	0.000982 ± 0.000189
05	0.00106 ± 0.000290	0.00135 ± 0.000317	0.00245 ± 0.000575	0.000651 ± 0.000136	0.000844 ± 0.000161	0.00138 ± 0.000271
06	0.00107 ± 0.000328	0.00147 ± 0.000421	0.00274 ± 0.000553	0.000887 ± 0.000352	0.00120 ± 0.000405	0.00214 ± 0.000582
09	0.00233 ± 0.000581	0.00321 ± 0.000868	0.00622 ± 0.00141	0.00277 ± 0.000476	0.00388 ± 0.000716	0.00821 ± 0.00128
10	0.00215 ± 0.000746	0.00287 ± 0.000991	0.00601 ± 0.00150	0.00159 ± 0.000598	0.00216 ± 0.000688	0.00517 ± 0.00240
11	0.00244 ± 0.000612	0.00332 ± 0.000944	0.00509 ± 0.00108	0.00282 ± 0.000958	0.00373 ± 0.00112	0.00629 ± 0.00137
12	0.00813 ± 0.00400	0.00994 ± 0.00421	0.0167 ± 0.00438	0.00624 ± 0.00216	0.00791 ± 0.00258	0.0136 ± 0.00381
13	0.00709 ± 0.00133	0.00929 ± 0.00183	0.0151 ± 0.00254	0.00749 ± 0.00170	0.00986 ± 0.00189	0.0160 ± 0.00237
14	0.00347 ± 0.000767	0.00411 ± 0.00997	0.00603 ± 0.00163	0.00337 ± 0.000800	0.00411 ± 0.00139	0.00629 ± 0.00225
Mean (n=11)	**0.00274 ± 0.00261**	**0.00353 ± 0.00314**	**0.00623 ± 0.00476**	**0.00243 ± 0.00237**	**0.00317 ± 0.00302**	**0.00569 ± 0.00490**

Table 5. AP COP excursions following balance perturbations for 11 participants. The perturbations occurred at time = 0 ms. Values are presented as mean ± standard deviation.

ID #	AP COP onset latency (ms)	AP COP peak latency (ms)	AP COP peak amplitude (cm)
02	206.87 ± 9.83	564.95 ± 94.32	13.65 ± 0.46
03	210.77 ± 8.12	552.55 ± 131.09	15.50 ± 1.40
04	199.84 ± 7.36	628.54 ± 151.49	13.28 ± 1.01
05	203.31 ± 7.88	607.89 ± 115.01	13.28 ± 0.73
06	227.29 ± 14.57	667.43 ± 162.29	15.75 ± 1.05
09	227.83 ± 8.81	569.31 ± 99.31	14.51 ± 1.28
10	224.44 ± 10.26	693.84 ± 178.54	10.40 ± 1.72
11	230.06 ± 12.24	622.85 ± 173.38	14.60 ± 1.42
12	223.29 ± 9.30	511.18 ± 38.35	13.93 ± 1.34
13	224.00 ± 11.79	498.84 ± 30.51	16.18 ± 1.65
14	205.31 ± 5.95	531.41 ± 154.23	10.17 ± 0.97
Mean (n=11)	**216.28 ± 14.61**	**586.14 ± 141.09**	**13.80 ± 2.20**

Table 6. Behavioural data for 11 participants during the flanker task. The button presses occurred at time = 0 ms. Values are presented as mean ± standard deviation.

ID #	*Reaction time (ms)			Error rate (%)	
	Congruent correct	Incongruent correct	Incongruent incorrect	Congruent	Incongruent
02	339.71 ± 56.61	373.69 ± 64.56	284.42 ± 51.76	10.90	21.04
03	335.48 ± 39.31	394.48 ± 46.40	320.29 ± 39.09	0.27	2.43
04	316.26 ± 60.58	341.43 ± 69.10	266.21 ± 43.79	5.51	17.15
05	308.11 ± 36.20	356.68 ± 51.84	289.46 ± 38.29	0.79	11.69
06	308.79 ± 49.18	340.24 ± 57.63	285.96 ± 34.92	14.00	26.11
09	301.18 ± 41.77	336.81 ± 44.87	268.15 ± 41.04	3.58	21.90
10	321.33 ± 48.34	369.99 ± 45.46	279.01 ± 47.20	2.75	32.38
11	330.02 ± 42.46	370.39 ± 39.55	306.24 ± 39.95	3.24	11.84
12	300.28 ± 36.53	373.82 ± 38.56	279.40 ± 31.10	1.10	29.35
13	312.09 ± 41.39	372.93 ± 43.98	280.56 ± 38.09	6.45	32.35
14	318.59 ± 46.67	343.30 ± 52.02	288.70 ± 44.99	10.11	20.32
Mean (n=11)	**315.93 ± 46.47**	**361.14 ± 56.50**	**281.72 ± 42.39**	**5.34 ± 4.57**	**20.60 ± 9.40**

* Too few errors occurred in the congruent trials to compute an average.

Electroencephalography

Cortical activity for each task condition was grand averaged (across trials for each participant and then across all participants). A clear N1 and ERN were evoked in response to perturbations during lean and release trials and errors made during the flanker task, respectively. For 11 participants at the FCz electrode location, the mean latency for the peak of the N1 was 107.91 ± 8.30 ms with a mean amplitude of 30.85 ± 10.95 μV (table 7). The mean latency for the peak of the ERN was 21.09 ± 16.39 ms with a mean amplitude of 10.35 ± 4.52 μV (table 7). Figures 4 and 5 show the grand averaged ERP waveforms for 11 participants during lean and release trials and flanker task, respectively. As demonstrated in figure 4, a clear ERN was evoked during the flanker task in response to error trials only. Too few errors were made on congruent trials to compute an average waveform. Figure 6 shows the corresponding two-dimensional

(2D) topographic map for each task, demonstrating negative activity in the fronto-central brain region.

Table 7. N1 and ERN latencies and amplitudes at the FCz electrode location for 11 participants prior to ICA for lean and release trials and erroneous trials in the flanker task, respectively. The perturbations and the button presses occurred at time = 0 ms.

ID #	N1		ERN	
	Latency (ms)	Amplitude (μV)	Latency (ms)	Amplitude (μV)
02	100.00	31.79	27.00	10.54
03	114.00	21.81	7.00	15.33
04	104.00	21.00	36.00	4.34
05	99.00	40.04	4.00	14.24
06	108.00	28.55	36.00	10.25
09	122.00	58.98	38.00	14.81
10	100.01	33.06	25.00	5.20
11	98.00	23.04	0.00	8.86
12	118.00	30.96	45.00	15.10
13	112.00	23.26	8.00	12.13
14	112.00	26.89	6.00	3.04
Mean (n=11)	**107.91 ± 8.30**	**30.85 ± 10.95**	**21.09 ± 16.39**	**10.35 ± 4.52**

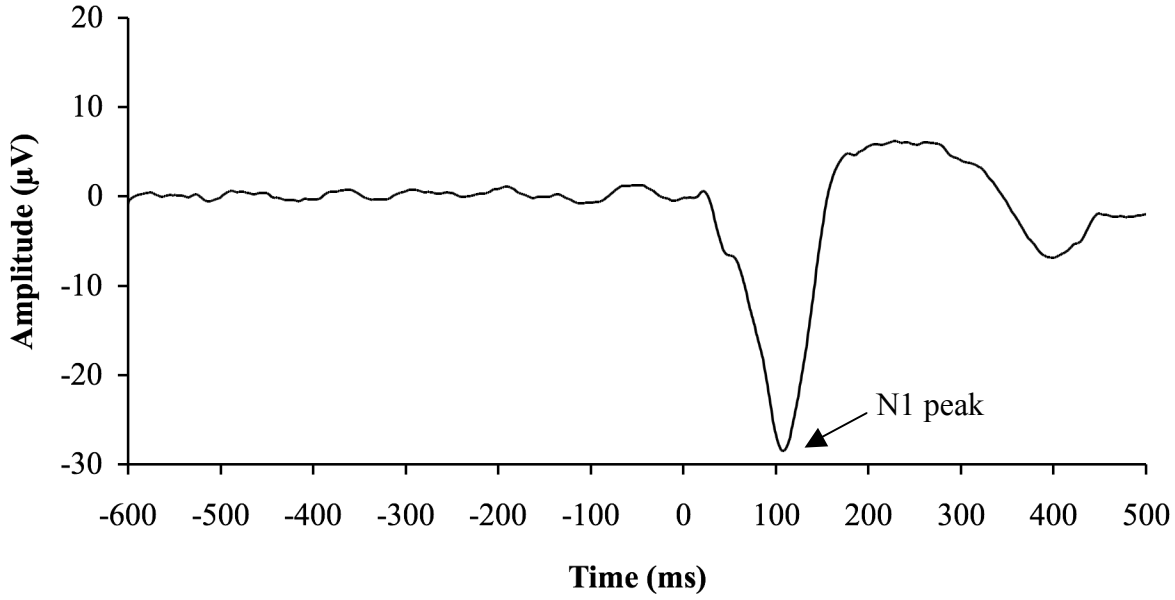

Figure 4. ERP waveform averaged across 11 participants for lean and release trials at the FCz electrode location prior to ICA. Time 0 corresponds to the onset of the perturbations.

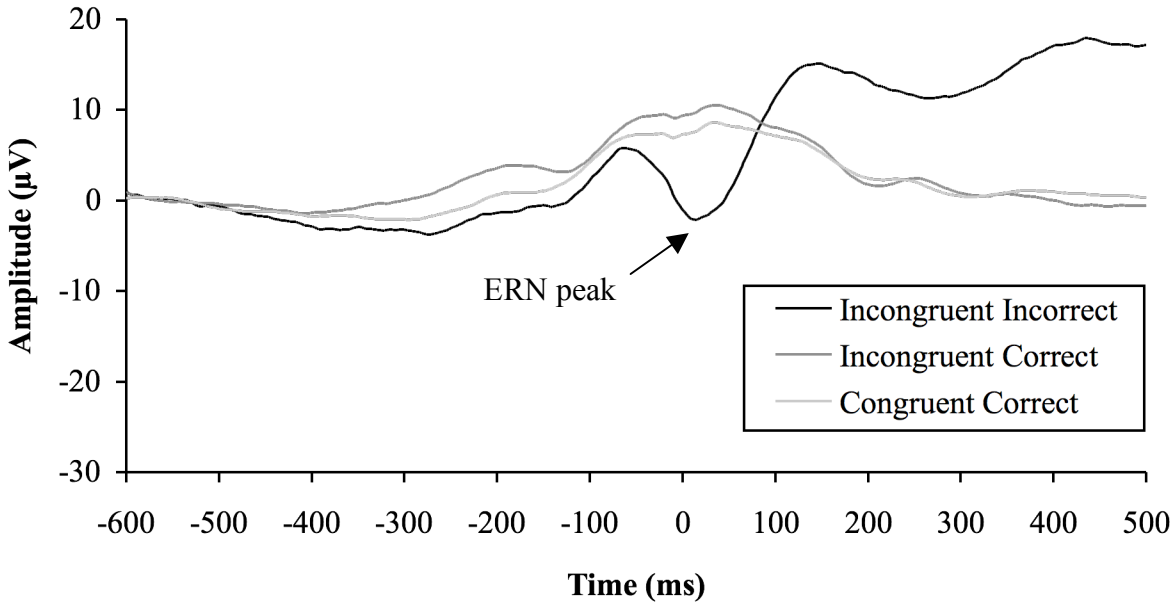

Figure 5. ERP waveforms averaged across 11 participants for the flanker task at the FCz electrode location prior to ICA. Time 0 corresponds to the time of the button presses.

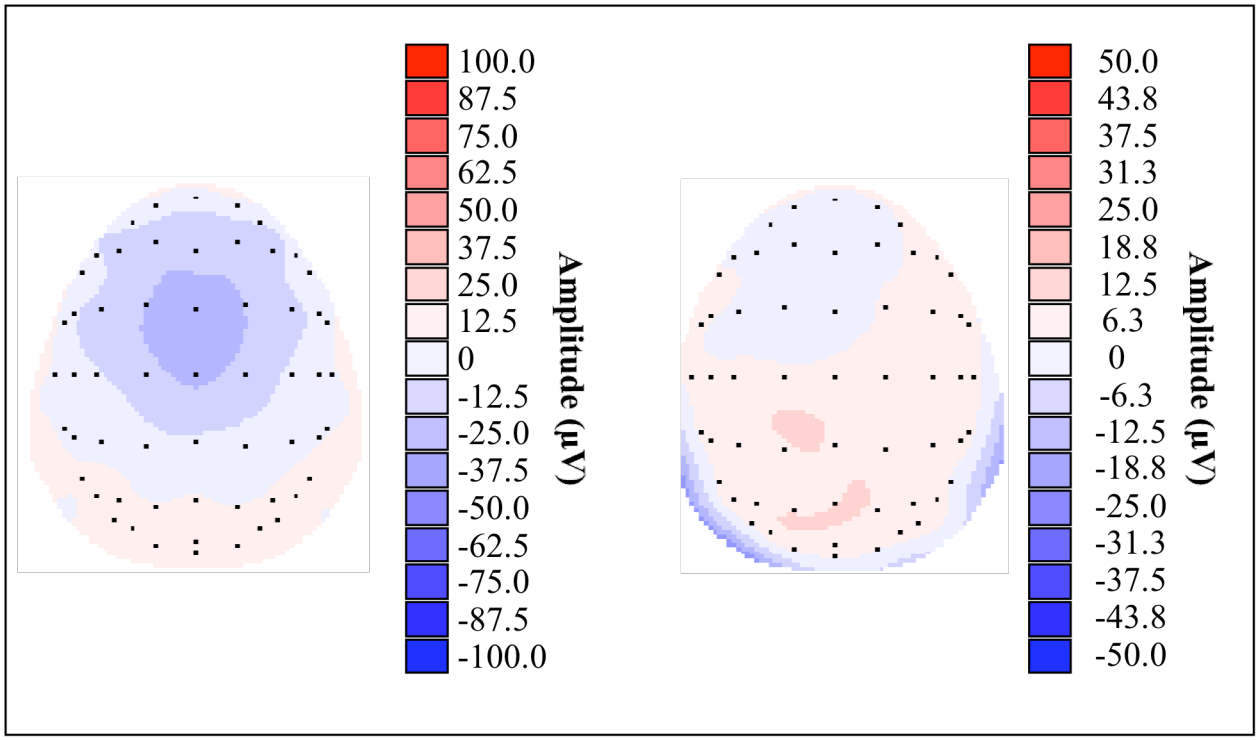

Figure 6. 2D topographic maps for the peak of the average N1 following perturbations (left) and the peak of the average ERN in response to errors in the flanker task (right) prior to ICA. The maps represent activity at the FCz electrode location for 11 participants.

Prior to source localization each participant's averaged N1 and ERN waveforms were additionally filtered using ICA. The ICA filtered data was then averaged across all 11 participants. Table 8 demonstrates the latencies and amplitudes of the N1 and ERN peaks for the ICA filtered data for each participant as well as the mean across all participants. For 11 participants at the FCz electrode location following ICA, the mean latency of the N1 peak was 103.00 ± 12.72 ms with a mean amplitude of 30.25 ± 9.05 μV. The mean latency of the ERN peak was 24.00 ± 16.82 ms with a mean amplitude of 16.06 ± 7.62 μV. The latency and amplitude shifts following the ICA may be attributed to the removal of ICA components that did not represent the potentials of interest (i.e., N1 and ERN). For example, removing noise components would have increased the SNR. Figures 7 and 8 show the grand averaged ICA filtered ERP waveforms for 11 participants during lean and release trials and the flanker task, respectively. Figure 9 shows the corresponding 2D topographic map for each task following ICA filtering, demonstrating a more profound negativity in the fronto-central region of the brain for the ERN following ICA (figure 9; right).

Table 8. N1 and ERN latencies and amplitudes at the FCz electrode location for 11 participants following ICA for lean and release trials and erroneous trials in the flanker task, respectively. The perturbations and button presses occurred at time = 0 ms.

ID #	N1		ERN	
	Latency (ms)	Amplitude (μV)	Latency (ms)	Amplitude (μV)
02	95.00	35.40	38.00	12.65
03	115.00	22.27	5.00	16.53
04	84.00	23.02	30.00	5.18
05	101.00	36.40	6.00	22.83
06	105.00	27.23	31.00	21.10
09	125.00	54.03	44.00	16.70
10	93.00	28.27	4.00	8.76
11	89.00	25.89	0.00	13.11
12	117.00	28.24	34.00	33.37
13	110.00	25.25	43.00	14.14
14	99.00	26.71	29.00	12.35
Mean (n=11)	**103.00 ± 12.72**	**30.25 ± 9.05**	**24.00 ± 16.82**	**16.06 ± 7.62**

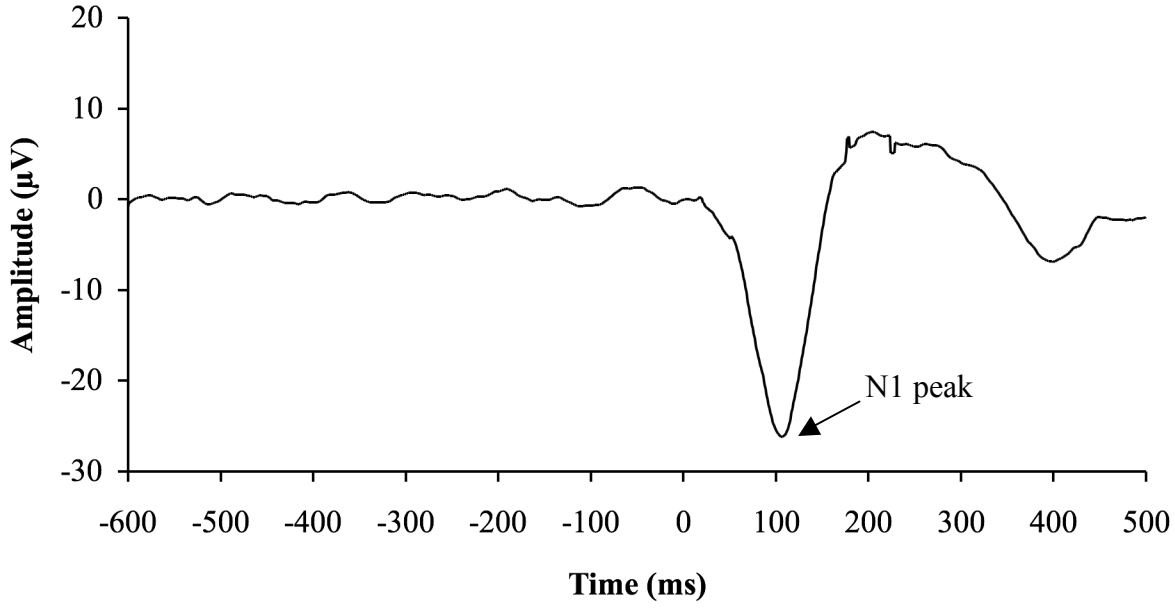

Figure 7. ERP waveform averaged across 11 participants for lean and release trials at the FCz electrode location following ICA. Time 0 corresponds to the onset of the perturbations.

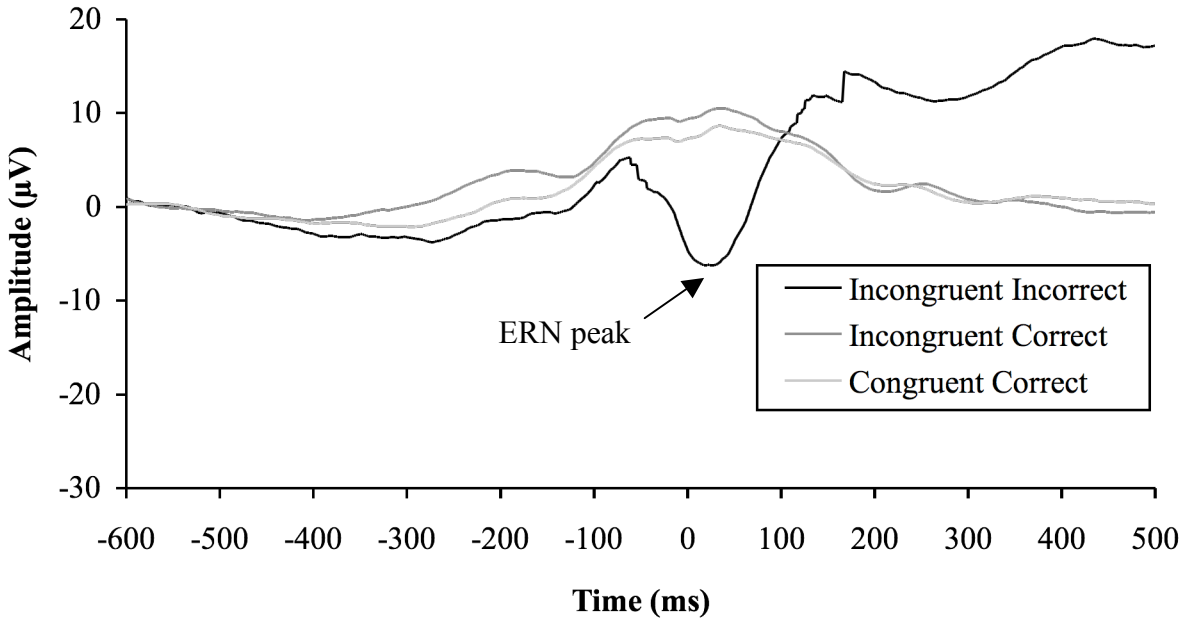

Figure 8. ERP waveforms averaged across 11 participants for the flanker task at the FCz electrode location following ICA. Time 0 corresponds to the time of the button press.

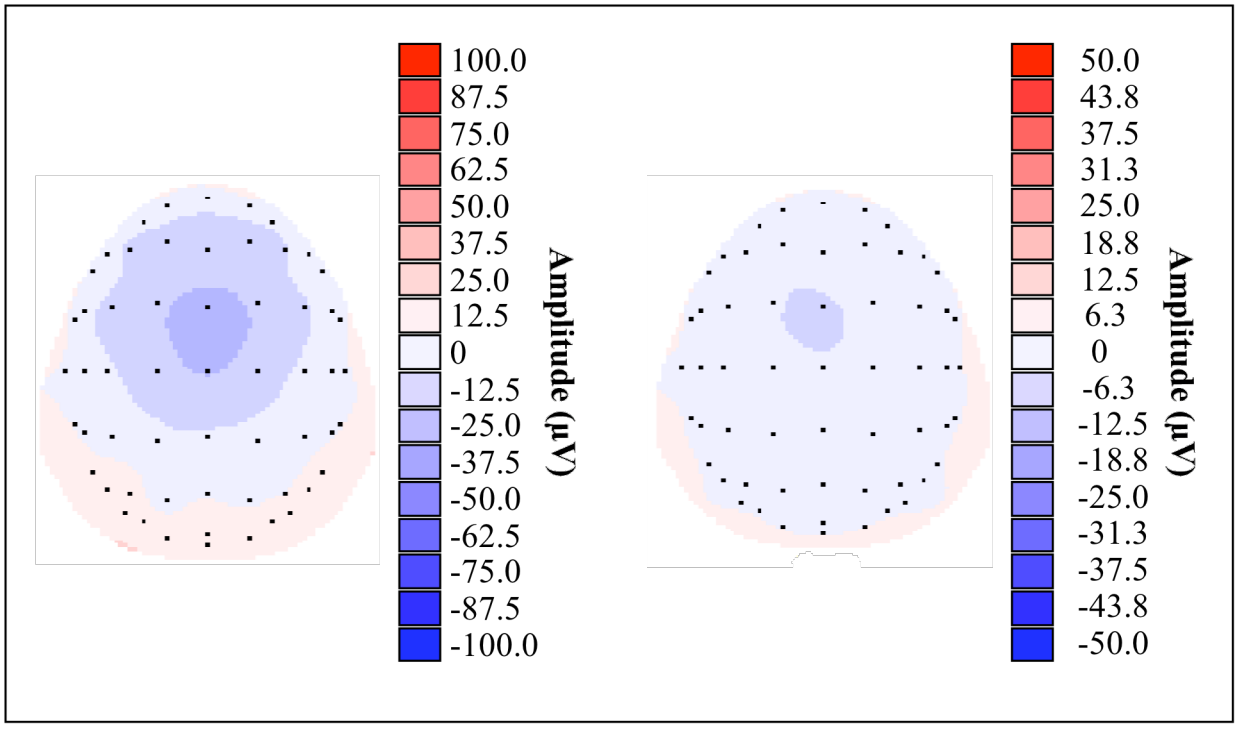

Figure 9. 2D topographic maps for the peak of the average N1 following perturbations (left) and the peak of the average ERN in response to errors in the flanker task (right) following ICA. The maps represent activity at the FCz electrode location for 11 participants.

Source Localization

One participant (ID# 04) was removed from source localization due to challenges in segmenting the cerebral cortex from their sMRI, rendering dipole analysis inaccurate. Dipole source localization was conducted for the 10 remaining participants. Noise estimation was performed for all 10 participants for an interval that had an average noise level of 0.65 ± 0.26 μV and 0.35 ± 0.14 μV across 10 participants for the balance and flanker EEG waveforms, respectively, and a maximum SNR of 28.00 ± 8.99 μV and 52.60 ± 41.68 μV across 10 participants for the balance and flanker EEG waveforms, respectively. Table 9 shows the Talairach coordinates and orientations of the N1 and ERN dipoles as well as the distance between dipoles for each of the 10 participants. Table 9 also reports the mean Talairach coordinates for each dipole across 9 participants. One participant (ID# 03) was removed from the mean for each dipole since their ERN dipole was located superior to the cerebral cortex, likely due to the fact that the participant very few error trials. The absolute value of the x coordinate for all participants was utilized when calculating the mean Talairach coordinates in order to have all dipoles located in the right cerebral hemisphere. Table 10 reports the N1 and ERN dipole Talairach labels (i.e., brain locations) for each of the 10 participants. The dipole results for one participant (ID# 13) are displayed in figure 10 for the N1 and figure 11 for the ERN. The dipole locations of the mean Talairach coordinates for the N1 and ERN across 9 participants are shown in figures 12 and 13, respectively (Talairach Daemon, Research Imaging Center, University of Texas Health Science Center, San Antonio, 2003).

Table 9. Talairach coordinates, orientations, and distance between N1 and ERN dipoles for 10 participants as well as the mean ± standard deviation across 9 participants (excluding participant 3).

ID #	Dipole Talairach coordinates & orientation (x, y, z)mm, (nx, ny, nz)		Distance between dipoles (mm)
	N1	ERN	
02	(3.2,-6.3,56.8)mm, (0.14,-0.82,-0.56)	(-12.9,11.9,42.6)mm, (-0.18,0.30,-0.94)	28.14
03	(2.8,-6.1,51.3)mm, (0.07,-0.92,-0.37)	(1.6,13.3,68.8)mm, (0.53,-0.76,0.39)	26.15
05	(11.7,-10.0,51.5)mm, (0.31,-0.14,-0.94)	(-2.8,-8.8,59.0)mm, (0.13,-0.79,-0.61)	16.37
06	(2.1,-14.9,57.1)mm, (-0.18,-0.82,-0.54)	(5.2,-12.4,43.0)mm, (-0.25,-0.50,-0.83)	14.65
09	(-12.3,-9.2,63.4)mm,(-0.28,-0.15,-0.95)	(5.4,-5.7,46.9)mm, (0.30,-0.51,-0.80)	24.45
10	(-4.7,11.9,44.0)mm, (-0.52,0.77,-0.36)	(-7.1,-19.7,37.4)mm, (0.24,-0.80,-0.55)	32.37
11	(6.3,-27.9,44.9)mm, (0.15,-0.88,-0.45)	(-7.3,-12.1,31.2)mm, (-0.17,-0.38,-0.91)	24.95
12	(-2.7,-16.8,64.0)mm, (-0.03,-0.68,-0.73)	(-4.2,-0.3,56.0)mm, (-0.13,-0.24,-0.96)	18.40
13	(5.0,-16.6,53.6)mm, (-0.15,-0.66,-0.74)	(9.1,20.9,28.2)mm, (0.31,0.16,-0.94)	45.48
14	(3.7,-16.5,48.3)mm, (0.10,-0.90,-0.42)	(-4.2,-13.5,26.2)mm, (-0.14,-0.56,-0.82)	23.66
Mean (n=9)	**(5.74±3.77, -11.81±10.84, 53.73±7.30)**	**(6.47±3.08, -4.41±13.15, 41.17±11.63)**	**25.46 ± 8.88**

Table 10. Talairach labels for the N1 and ERN dipoles for 10 participants.

ID #	Talairach label	
	N1	ERN
02	Medial frontal gyrus; Brodmann area 6	Medial frontal gyrus; Brodmann area 32
03	Medial frontal gyrus; Brodmann area 6	No location reported
05	Medial frontal gyrus; Brodmann area 6	Medial frontal gyrus
06	Medial frontal gyrus; Brodmann area 6	Paracentral lobule; Brodmann area 31
09	Medial frontal gyrus; Brodmann area 6	Cingulate gyrus; Brodmann area 24
10	Medial frontal gyrus; Brodmann area 6	Cingulate gyrus
11	Paracentral lobule	Cingulate gyrus
12	Medial frontal gyrus	Medial frontal gyrus; Brodmann area 6
13	Medial frontal gyrus	Cingulate gyrus
14	Medial frontal gyrus	Cingulate gyrus; Brodmann area 23

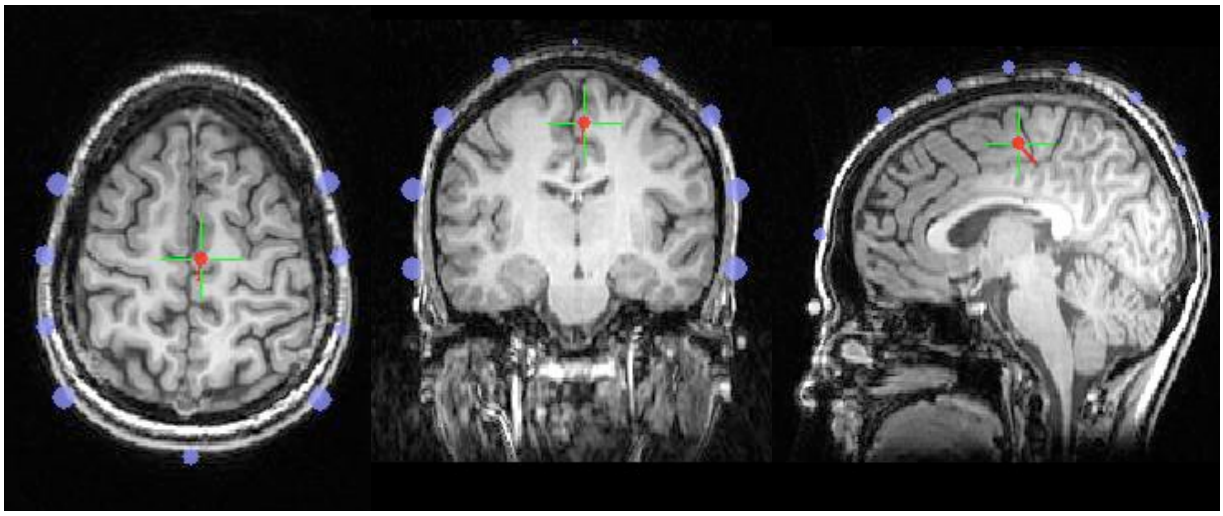

Figure 10. Axial (left), coronal (centre), and sagittal (right) image results of the single fixed coherent dipole for the N1 for one participant (ID# 13). The dipole was located in the medial frontal gyrus with Talairach coordinates of (5.0, -16.6, 53.6) mm and an orientation of (-0.15, -0.66, -0.74).

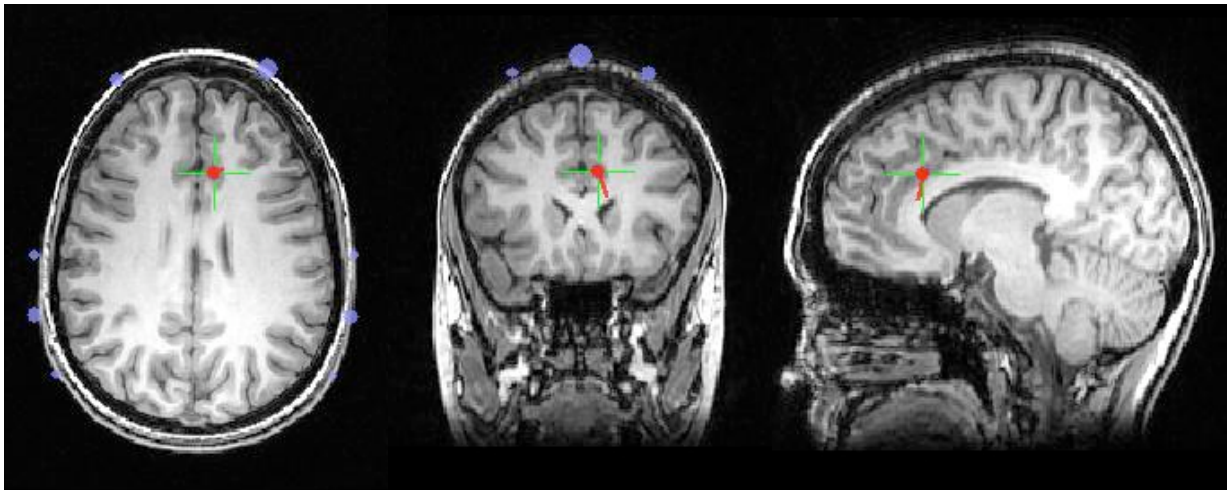

Figure 11. Axial (left), coronal (centre), and sagittal (right) image results of the single fixed coherent dipole for the ERN for one participant (ID# 13). The dipole was located in the cingulate gyrus with Talairach coordinates of (9.1, 20.9, 28.2) mm and an orientation of (0.31, 0.16, -0.94).

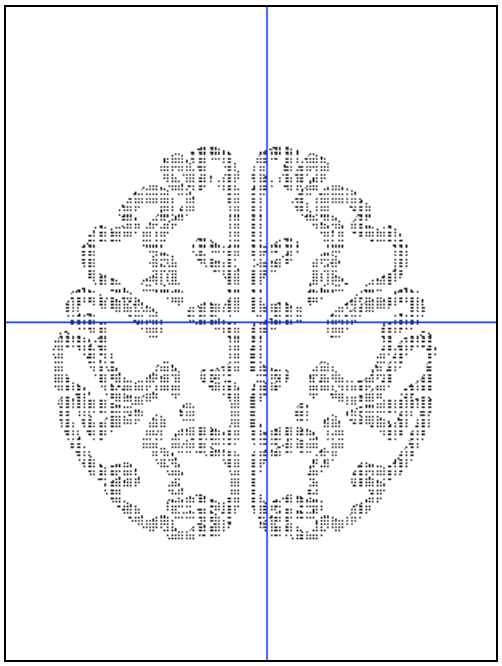

Figure 12. An axial slice where the crosshair point of intersection represents the N1 dipole location for the mean (n=9) Talairach coordinates (5.74, -11.81, 53.73) mm. These coordinates corresponded to the medial frontal gyrus (Brodmann area 6).

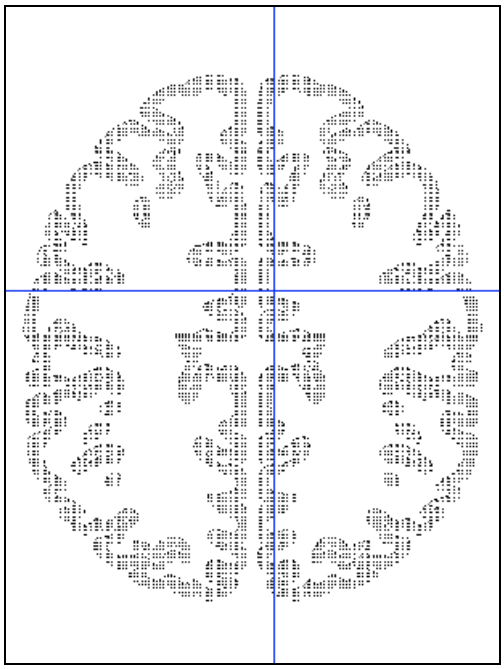

Figure 13. An axial slice where the crosshair point of intersection represents the ERN dipole location for the mean (n=9) Talairach coordinates (6.47, -4.41, 41.17) mm. These coordinates corresponded to the cingulate gyrus (Brodmann area 24).

DISCUSSION

The overall objective of the present research was to provide a more detailed understanding of the specific neurophysiologic events that occur at the cortex following a balance disturbance. More specifically, the focus of this study was to determine whether the perturbation-evoked N1 response has a parallel cortical representation to the error detection related ERN evoked during a cognitive task. Such a parallel would have revealed that the N1 might be associated with an error detection mechanism. We were able to evoke typical behavioural and electrophysiological responses during the lean and release task and the flanker task. However, in contrast to the main hypothesis, the present results revealed that the dipole location of the N1 was not similar to that of the ERN. The mean distance between the N1 and ERN dipoles across participants was 25.46 ± 8.88 mm, which is greater than the average EEG source localization error of 10.5 ± 5.4 mm determined by Cuffin et al. (2001). We speculate that the distance between the dipoles in the present study is too large to be explained by factors contributing to localization error and, thus, conclude that the negativities have different neural generators. The source localization for the mean ERN dipole corresponded to the cingulate gyrus (Brodmann area 24), which represents the ACC (Martin, 2003). This observation supports results from previous literature (Badgaiyan & Posner, 1998; Carter et al., 1998; Carter et al., 2001; Dehaene et al., 1994; Gehring, 1992; Gemba et al., 1986; Holroyd et al., 1998, 2004; Kerns et al., 2004; Kiehl et al., 2000; Menon et al., 2001; Miltner et al., 1997, 2003; Niki & Watanabe, 1979; Shima & Tanji, 1998; Ullsperger & von Cramon, 2003). However, the source localization for the mean N1 dipole corresponded to the medial frontal gyrus (Brodmann area 6), rather than the originally hypothesized ACC. This leads to the conclusion

that the perturbation-evoked N1 differs in its potential role from the ERN recorded during the flanker task. The electrophysiological and behavioural data are addressed to determine whether the responses evoked were typical of previous studies. This is followed by a discussion of the potential interpretation of the measured differences in source localization between these two tasks.

Electroencephalography

The polarity, latency, amplitude, and topographic representation of the peak of the N1 measured during the balance reactions were comparable with those reported in literature (Dietz et al., 1984; Dietz, Quintern, & Berger, 1985; Dietz, Quintern, Berger, & Schenck, 1985; Dimitrov et al., 1996; Duckrow et al., 1999; Quant, Adkin, Staines, Maki, et al., 2004; Quant, Adkin, Staines, & McIlroy, 2004; Staines et al., 2001). The consistency of this potential across such a range of different perturbation conditions (e.g., Adkin et al., 2006; Dietz et al., 1984; Dietz, Quintern, & Berger, 1985; Dietz, Quintern, Berger, & Schenck, 1985; Mochizuki et al., 2008, 2010; Mochizuki, Sibley, Cheung, & McIlroy, 2009; Mochizuki, Zabukovec, et al., 2009; Staines et al., 2001; Quant, Adkin, Staines, Maki, et al., 2004; Quant, Adkin, Staines, & McIlroy, 2004; Quintern et al., 1985) speaks to the robust nature of this potential. Note that similar to previous work, the N1 represents a very large amplitude signal (often greater than 50 μv), which likely maximized the ability to localize the source dipole due to an excellent SNR. Thus, we are most certainly confident in the results of the source localization for the N1 due to the excellent SNR properties.

In contrast, while the polarity, amplitude, and topographic representation of the ERN evoked in this study during the flanker task were similar to other studies, the latency of the ERN peak was shorter in the present study (21.09 ± 16.39 ms following the onset of the error) compared to what is typically found in literature (50-150 ms following the onset of the error) (Falkenstein et al., 1990; Gehring et al., 1990, 1993; Gemba et al., 1986; Miltner et al., 2003; Sasaki & Gemba, 1986). We were unable to account for such differences due to any technical problems; therefore, we speculate that the discrepancy in timing is due to the fact that we do not have an accurate measure of when the error actually occurred. The ERP waveform is time-locked to the mouse button press, which captures when the response was executed, but does not capture the exact timing of the error or the time of realization that an error was made. Anecdotal feedback from participants indicated that the time of realization of an error varies. On some trials the participants knew they were making an error before the button had been pressed and on other trials they did not realize an error was made until after the button was pressed. A discrepancy in reaction times, particularly slower, was also considered for explaining why the ERN latency was more rapid than that found in the literature. However, the reaction times reported in table 6 are comparable to those reported by Ullsperger & von Cramon (2001) for a flanker task with the same timing parameters.

The inability to time lock the ERP analysis to the exact onset of the event could result in a poor SNR, possibly explaining why the amplitude of the ERN is small compared to the N1 that is time-locked to the stimulus. This is not a concern in the lean and release trials because the exact timing of perturbation onset was recorded (onset of cable release) and the balance response is tightly coupled to the onset of the stimulus. Thus, the amplitude of the signal and

the SNR of the N1 are larger compared to the potentials linked to the ERN. As evident from the 2D topographic maps at the peak of the ERN (figures 6 and 9), there is a negativity of small amplitude concentrated in the fronto-central region of the brain, corresponding to the topographic representation of the ERN cited in literature (Falkenstein et al., 1990; Gehring et al., 1990, 1993; Gemba et al., 1986; Miltner et al., 2003; Sasaki & Gemba, 1986). Overall, we were successful in evoking electrophysiological responses that were consistent with previous literature. Importantly, the differences in the ERN latency did not appear to influence the topographic representation and associated source localization.

Behavioural Data

The behavioural results (i.e., EMG and AP COP) for the balance task revealed that the lean and release protocol reliably evoked feet-in-place compensatory balance reactions with characteristics comparable to those reported in literature (e.g., Adkin et al., 2006; Mochizuki et al., 2008). The EMG and COP onset latencies were slower than some previous work, most likely due to the smaller amplitude of perturbation used in this study. The amplitude of the perturbation is associated with the initial lean angle and in this study we set out to limit the compensatory balance reactions to feet-in-place responses, requiring a relatively small initial lean angle and resulting in a slow initial acceleration after the onset of the perturbation. As a result, the amplitude of the perturbation was smaller than studies such as Mochizuki et al. (2010) who focused on stepping reactions. However, our data is in line with the work of Adkin et al. (2006) who focused on smaller amplitude perturbations. Overall, the characteristics of the evoked balance reactions were consistent with comparable feet-in-place reactions evoked

in other studies, indicating that any differences in the underlying source localization were not attributable to unique characteristics of the evoked balance reactions.

As stated previously, the reaction times for the flanker task were comparable to those reported by Ullsperger & von Cramon (2001) for a flanker task with the same timing parameters. The mean reaction times for the present study were 315.93 ± 46.47 ms for congruent correct trials, 361.14 ± 56.50 ms for incongruent correct trials, and 281.72 ± 42.39 for incongruent incorrect trials. Similarly, in the study by Ullsperger & von Cramon (2001), the mean reaction times were 323 ± 6.80 ms for congruent correct trials, 378 ± 6.10 ms for incongruent correct trials, and 283 ± 7.90 ms for incongruent incorrect trials. Consistent with the previous study, since error rates were higher and reaction times were longer for incongruent trials, it demonstrates that participants had more difficulty with the trials with a higher response conflict (Ullsperger & von Cramon, 2001). Research has demonstrated that every incongruent trial during the flanker task generates both an incorrect and correct response, resulting in response conflict (Gratton et al., 1988, 1992 in Ullsperger & von Cramon, 2001). Ullsperger and von Cramon (2001) suggested that in order to resolve this conflict and subsequently generate the correct response, the conflict must be detected and the incorrect response must be inhibited. Presumably, this process involved with high response conflict requires time, resulting in a longer reaction time for incongruent trails as compared to trials with lower response conflict (i.e., congruent trials). It is speculated that error trials consistently produce the fastest reaction times due to failure to detect response conflict and subsequently inhibit the incorrect response. Overall, the parallels in the behavioural data support the

similarities in electrophysiology and source localization, confirming that the evoked negativity is consistent with the previously described ERN.

Interpreting the dipole location: ERN versus the perturbation-evoked N1 response

As noted previously, the behavioural and electrophysiological data revealed that we had success in evoking the respective reactions and underlying CNS control for the N1 and ERN. However, the source location revealed a different underlying dipole (ACC for the ERN and Brodmann area 6 for the N1). This difference has countered the original hypothesis that the N1 is analogous to the ERN. The question becomes, what is the potential interpretation of the N1 in light of a source localized to the medial frontal gyrus (Brodmann area 6)?

Brodmann area 6 is comprised of two premotor cortical regions, the premotor cortex laterally and the SMA medially. The premotor regions are known to integrate sensory information from association cortices and subcortical regions in order to form movement plans, as they project to the primary motor cortex and represent the site of origin for the corticospinal tract (Martin, 2003). The corticospinal tract is responsible for sensory control and voluntary movement of limb and axial muscles (Martin, 2003). Based on the resulting mean Talairach coordinates, (5.74, -11.81, 53.73) mm, and the corresponding Talairach label, medial frontal gyrus (Brodmann area 6), of the N1 dipole in the present study, it is speculated that the generator of the N1 is the SMA. The SMA receives its major projections from the basal ganglia, subcortically, via the ventral anterior nucleus of the thalamus, as well as from the prefrontal cortex, which is involved in higher-level planning of movements (Martin, 2003).

In accordance with the known function of the premotor cortical regions (i.e., integration of sensory information from association cortices and subcortical regions), it could be thought that the N1 represents sensory processing of the balance perturbation. However, as stated previously, Mochizuki and colleagues (2008) demonstrated that the amplitude of the N1 is strongly influenced by the temporal predictability of the perturbation, independent of the evoked sensory discharge linked to the perturbation. When the perturbation magnitude was held constant (i.e., providing the exact same amount of sensory input across perturbations), the ability to predict the onset timing of the perturbation attenuated the N1 amplitude, as compared to temporally unpredictable perturbations (Mochizuki et al., 2008). It has been speculated that an earlier evoked potential, the P1, which occurs approximately 40-50 ms following the onset of the perturbation, in fact represents the sensory information of the perturbation since its maximum amplitude is topographically located over the primary sensory cortex (Jacobs & Horak, 2007). Also, the integration of the perturbation related sensory information (e.g., visual, vestibular, and somatosensory) is thought to occur over a distributed network involving the temporal, parietal, and insular cortices (Blanke, Perrig, Thut, Landis, & Seeck, 2000; Brandt, Dieterich, & Danek, 1994; de Waele, Baudonnière, Lepecq, Tran Ba Huy, & Vidal, 2001; Jacobs & Horak, 2007; Johannsen, Broetz, Naegele, & Karnath, 2006; Perennou et al., 2000). Thus, it is evident that the N1 does not simply represent the sensory processing of the perturbation.

It would seem reasonable to propose that the N1 is linked to the execution of the motor response to counteract the loss of stability with an SMA generator since the premotor regions are expected to play a role in the execution of movements due to their direct projections to the

spinal cord via the corticospinal tract (Martin, 2003). However, based on the results of the ankle pendulum study by Quant, Adkin, Staines, and McIlroy (2004), it was concluded that the N1 is not linked to the execution of motor responses. To reiterate, Quant, Adkin, Staines, and McIlroy (2004) compared N1 responses when participants were asked to either react or not react to the perturbation (active versus passive), and discovered that large amplitude N1 responses were apparent even when compensatory balance reactions were absent. Therefore, the N1 cannot represent the execution of motor responses since there was no muscle activity. Further evidence countering the idea that the N1 represents the execution of the motor response comes from the comparison of the present study to previous work. The timing of the peak N1 remains relatively consistent across different perturbation amplitudes, directions, and initial positions of the individual, despite the fact that the onset latencies of the compensatory muscle activity and COP excursions vary substantially. For example, the N1 peak latencies following the perturbation between the present study (107.91 ± 8.30 ms) and the 2010 study by Mochizuki and colleagues (block unconstrained = 97.8 ± 11.6 ms; block constrained = 94.3 ± 14.0 ms; random unconstrained = 100.6 ± 12.0 ms; random constrained = 101.9 ± 13.1 ms) are very similar despite the large differences in EMG and COP onset latencies between the studies. This further suggests that the N1 has little to do with the initial motor execution of the compensatory response. Also, the fact that the peak N1 does not consistently precede the onset of the motor response may suggest that the N1 contributes to the planning of the later phases of the compensatory response.

Compensatory balance responses consist of different phases. The initial, short-latency phase of the compensatory balance response is automatic (Jacobs & Horak, 2007; McIlroy et

al., 1999) and is composed of automatic spinal reflexes, which briefly activate distal leg muscles (Ackermann, Dichgans, & Guschlbauer, 1991). However, since these reflexes are inadequate for regaining stability (Jacobs & Horak, 2007), peripheral sensory information evoked by the balance disturbance consecutively elicits pre-set synergies that are stored within the brainstem that activate stabilizing muscles throughout the body (Horak & Nashner, 1986; Nashner, 1976). There is substantial evidence to support the claim that the early phases of the medium- and long-latency components of the balance response do not include transcortical loops (e.g., Ackermann et al., 1991; Berger, Horstmann, & Dietz, 1990; Dietz et al., 1984; Dietz, Quintern, Berger, & Schenck, 1985; Honeycutt & Nichols, 2006; Quintern et al., 1985). It was demonstrated by McIlroy et al. (1999) that only the later phases of the compensatory balance response require attentional resources (i.e., involvement of the cortex), as attentional shifts away from a dual task only occurred approximately 200-300 ms following the onset of the balance reaction, which began approximately 90 ms following the onset of the perturbation. Thus, it appears that it is only the later phases of compensatory balance responses that involve the cerebral cortex and that can be modified to fit the characteristics of the perturbation, the environmental surround, and the intentions of the individual (Beloozerova et al., 2003, 2005; Burleigh & Horak, 1996; Chan, Melvill Jones, Kearney, & Watt, 1979; Norrie et al., 2002; Taube et al., 2006).

It has been suggested that feet-in-place reactions are pre-set synergies stored and executed subcortically in order to attempt to restabilize following a balance disturbance, and that change-in-support reactions are generated within the cortex if the feet-in-place reaction is not adequate (Jacobs & Horak, 2007; Quintern et al., 1985). However, change-in-support

strategies start as early as 120 ms following the onset of the perturbation in a tilting chair (Gage, Zabjek, Hill, & McIlroy, 2007; Mochizuki, Sibley, Cheung, Camilleri, et al., 1999; Sibley, Lakhani, Mochizuki, & McIlroy, 2010). Thus, like feet-in-place strategies, change-in-support strategies may also be initiated by spinal reflexes and pre-set synergies within the brainstem, however, the characteristics of the response (i.e., proper trajectory, amplitude of the response or distance of the step or reach, etc.) may be shaped by the cortex in the later phases of the reaction based on the characteristics of the perturbation and the environmental surround (i.e., place a safe step or grab a stable object) (Ghafouri, McIlroy, & Maki, 2004; Jacobs & Horak, 2006; Tripp, McIlroy, & Maki, 2004; Zettel, Holbeche, McIlroy, & Maki, 2005; Zettel, McIlroy, & Maki, 2002a,b). Thus, the N1 may represent the SMA's participation in generating a contingency motor plan to shape the later phases of the compensatory balance reaction in anticipation of the initial attempts by the pre-set brainstem synergies being inadequate. Based on the evidence that the SMA plays a role in the planning of internally generated voluntary movements (Martin, 2003) and the suggestion by Jacobs and Horak (2007), due to results of previous research (e.g., Hanakawa, Fukuyama, Katsumi, Honda, & Shibasaki, 1999; Jacobs & Horak, 2006; Jobges et al., 2004; Rogers, Johnson, Martinez, Mille, & Hedman, 2003), that voluntary and compensatory stepping are governed by the same underlying cortical-brainstem circuits, the SMA could potentially play a role in the planning or shaping of the later phases of externally generated compensatory movements. Literature has shown that the later phases of compensatory balance reactions are executed by the primary motor cortex (Bard, 1933 in Jacobs & Horak, 2007; Beloozerova et al., 2003; Taube et al., 2006), which projects fibres that make up the majority of the corticospinal tract (Martin, 2003). The SMA may automatically generate these contingency plans in response to balance disturbances and project them to the

primary motor cortex via their substantial connection fibres (Martin, 2003). The primary motor cortex, in turn, may only execute these plans based on the necessity of the movement or the individual's intention to move or not move if the disturbance in not overly threatening. Evidence from Burleigh and Horak (1996) and Norrie et al. (2002) suggests that a balance response can be modified by the individual's intentions. In the case of the study by Quant, Adkin, Staines, and McIlroy (2004), the participants were not exposed to a threatening perturbation. They knew prior to the perturbation that they would not lose stability from a tilting ankle platform while sat in a stable chair. Based on internal information about past experiences as well as external cues informing them about the environment and the threat of the perturbation, they were able to pre-select the appropriate response (Jacobs & Horak, 2007) and inhibit the compensatory balance reaction, as evident from the lack of EMG activity post-perturbation.

Further evidence supporting the suggestion that the N1 represents the planning of the later stages of the compensatory response based on what is required to regain stability comes from the fact that the timing of the N1 remains consistent (Mochizuki et al., 2010; Mochizuki, Sibley, Cheung, Camilleri, et al., 2009; Quant, Adkin, Staines, & McIlroy, 2004) while the amplitude of it scales to the temporal predictability of the perturbation (Adkin et al., 2006; Mochizuki et al., 2008) and the consequence, such as the size of the perturbation (Camilleri, Sibley, Zabjek, & McIlroy, 2006; Mochizuki et al., 2010; Staines et al., 2001). This could relate to the amount of planning that needs to be done or the number of resources that need to be recruited in order to regain stability. Previous studies have shown that the amplitude of the N1 is affected by the temporal predictability of the perturbation. While Adkin et al. (2006)

demonstrated that the N1 is completely abolished when the perturbation was temporally predictable, other studies have demonstrated that the relative amplitude is, rather, attenuated (Mochizuki et al., 2008, 2010). In a predictable perturbation, preparatory cortical activity begins prior to the onset of the perturbation (Jacobs et al., 2008; Maeda & Fujiwara, 2007, Mochizuki et al., 2008, 2010; Yoshida, Nakazawa, Shimizu, & Shimoyama, 2008) as demonstrated by a negative slow-wave DC shift in the EEG waveform beginning as early as approximately 1200 ms prior to the onset of the perturbation (Mochizuki et al., 2008, 2010). Since the pre-perturbation preparatory activity (Jacobs et al., 2008; Mochizuki et al., 2008, 2010) and the N1 (Dimitrov et al., 1996; Duckrow et al., 1999; Quant, Adkin, Staines, & McIlroy, 2004) are maximal over the same electrode site it could be thought that a relationship exists between their underlying cortical processes. However, Mochizuki and colleagues (2010) demonstrated that the pre-perturbation preparatory activity of the cerebral cortex and the post-perturbation N1 are independent components. The negative shift prior to the onset of the perturbation represents the modification of central set (i.e., state of the CNS) based on the context of the upcoming perturbation (i.e., predicted consequence) in order to evoke the optimal response (Mochizuki et al., 2008, 2010). This was evident based on the scaling of the amplitude of the pre-perturbation cortical activity when the size of the perturbation was known to the participant (Mochizuki et al., 2010). When the size of the perturbation was unknown to the participant, a consistently large pre-perturbation amplitude was apparent, which was suggested to represent recruiting more resources to prepare for the worst possible outcome of the perturbation (Mochizuki et al., 2010). This preparatory cortical activity occurs in the absence of preparatory postural muscle activity, demonstrating that it relates to planning or the

modification of central set within the cortex to optimize the balance response and minimize the expected consequence of the perturbation (Mochizuki et al., 2008, 2010).

Some planning of the later phases of the compensatory response still needs to occur after the perturbation in order to accurately react to regain stability based on the sensory feedback of the actual characteristics (i.e., consequence) of the perturbation. It is speculated that the N1 amplitude is attenuated in predictable perturbations because modifications to central set, in order to generate optimal reactions, occurred prior to the perturbation based on the perceived amount of threat. Therefore, the amount of cortical activity required following the perturbation is reduced (Mochizuki et al., 2008). In other words, the SMA has less work to do in planning the later phases of the compensatory response. This decrease in N1 amplitude is also seen when the amplitude of the perturbation is smaller (Staines et al., 2001), indicating that less planning for modification of the later phases of the response is needed when there is less threat. Despite the fact that the preparatory cortical activity modifies central set to generate optimal responses based on past experiences or current context, the amplitude of the N1 always scales to the amplitude of the perturbation (Mochizuki et al., 2010). This coincides with the speculation that the SMA generates a plan for the later phases of the response automatically based on sensory feedback from the perturbation in case the initial responses generated are not adequate to regain stability. This was evident in the study by Mochizuki et al. (2010) when there was no difference in the amplitude of the N1 for the large perturbation whether the size of the perturbation was known or not known. Mochizuki et al. (2010) speculated that the size of the perturbation (i.e., consequence) was larger than the modification in central set prior to the perturbation, demonstrating that planning based on the consequence of the perturbation still

needs to be done in case the optimal response based on the context is not sufficient. In the study by Mochizuki et al. (2010), the timing of the perturbation onset was always known, which could contribute to why the amplitude of the N1 did not change across large perturbation conditions. Unpredictable perturbations should have been introduced in order to determine if the size of the N1 was attenuated in the temporally predictable conditions.

Mochizuki et al. (2010) suggested that when the threat of the postural instability is greater, preparatory activity and post-perturbation cortical responses are independent, whereby the former attempts to modify the state of the CNS to optimize the forthcoming compensatory response based on the context or expected outcome of the perturbation and the latter creates a plan to optimize the later phases of the compensatory response based on the actual consequence of the perturbation. Mochizuki et al. (2010) demonstrated that the balance responses were in fact optimized, based on the scaling of the EMG amplitude to the size of the perturbation regardless of whether the size of the perturbation was known prior to its onset (i.e., EMG amplitude did not scale to the size of the preparatory cortical activity). This indicates that the optimal response is dependent upon both the preparatory activity and the N1, even though they may represent different underlying processes, since the post-perturbation response is more accurate due to sensory feedback from the perturbation (Dietz et al., 1984; Dietz, Quintern, Berger, & Schenck, 1985). While Mochizuki et al. (2010) determined that pre- and post-perturbation cortical events are independent processes; future research should focus on the source localization of the preparatory cortical activity to determine whether it has a different generator than the N1. This would provide further insight into their degree of independence.

Limitations

There are limitations in the present study that need to be addressed. The first limitation involved defining the segmentation thresholds for each individual's sMRI within the source localization software (CURRY). Depending on the quality of the image it was difficult to accurately differentiate between layers (i.e., white matter, grey matter, brain, and skin). This was the reason for the exclusion of one participant from the dipole analysis. While it was possible to differentiate the layers in the participants included in the dipole analysis, it is not possible to be 100% confident that there was no overlap between the layers. This could have resulted in some error in the construction of the 3D realistic models of the cortex and the head and, therefore, could have lead to error in the localization of the dipole.

A second limitation within CURRY was the co-registration of the electrode positions and the sMRI for each participant. Although the 3D electrode positions were recorded during data collection, the electrode positions appeared warped when they were coregistered to the 3D model of the cortex. In order to avoid the warping of the electrode positions, the electrodes were aligned to the 10-20 system to correspond with the electrode placement during collection. This could have also lead to some discrepancy in the source localization.

Another possible limitation in the present study is the use of a single dipole model for representing the activation for the N1 and ERN. It is difficult to know for certain whether these negativities have one generator or whether they are the result of activity across a distributed cortical network. However, it has been shown that a single dipole model is appropriate for the ERN (Dehaene et al., 1994; Holroyd et al., 1998). In the present study, multiple dipoles were

tested for each participant for both negativities. One dipole remained stable in the location determined by the single dipole model, whereas additional dipoles were localized to areas that were not plausible sources (e.g., skull, ventricles, etc.). Thus, the single dipole model was appropriate for the present data for the time window of interest.

A limitation of the dipole source localization method in general involves the inverse problem. EEG measures activity from the entire surface area of the head, encompassing activity from all aspects of the brain. The electrical signlas from deeper structures get "smeared" while traveling, via volume conduction, through the cerebrospinal fluid, multiple brain structures, skull, and scalp. While CURRY attempts to solve the inverse problem and localize the generator deep within the cortex, it cannot be solved entirely. ICA, utilized prior to source localization in the present study, also attempts to solve the inverse problem by identifying independent components in the EEG waveform of interest. However, there are inherent limitations with ICA. ICA may not isolate components from single neural sources since a large number of cortical areas are likely active during the time window of interest. Attempts were made in the present study to control for this limitation by focusing the ICA time window around the N1 and ERN only and by selecting components that represented the characteristics of the waveform of interest. Another limitation with ICA is that the selection of components is largely subjective. Steps were taken to generate rules for inclusion and exclusion of ICA components in order to ensure that decisions were consistent across participants.

A final limitation is ecological validity. The perturbations evoked in this study may not be representative of balance disturbances that occur in every day life when considering the lean angle, harness, cable system, as well as the general laboratory setting. The same concern exists with the flanker task. However, the purpose of this study was not to mimic a real world experience but rather to probe cortical processes. Despite the limitations of the present study, the results provide some insight into the cortical control of compensatory balance responses.

Conclusion

In summary, the results of this study revealed that the dipole location of the activation following the balance disturbance (N1) was not similar to that evoked following errors in the flanker task (ERN). Similar to previous research, the source localization for the mean ERN dipole corresponded to the cingulate gyrus (Brodmann area 24), which represents the ACC. However, the source localization for the mean N1 dipole corresponded to the medial frontal gyrus (Brodmann area 6), rather than the originally hypothesized ACC. This leads to the conclusion that the negativities do not have the same underlying circuitry, revealing that the N1 may not be linked to the same error detection mechanism as the ERN. It is speculated that the generator of the N1 is the SMA and that it represents the generation of a contingency motor plan in order to shape the later phases of the compensatory balance response based on sensory feedback from the perturbation.

Although the results of the present study do not apply directly to the clinical population, advancing the understanding of the neural control of compensatory balance in the healthy population has potential future application to advancing diagnostic and/or

rehabilitation strategies for individuals with neurological injuries (e.g., stroke) who experience compromised balance control. Future research should focus on developing a greater understanding of the underlying function of the perturbation-evoked N1 response in light of a sourced localized to the SMA.

REFERENCES

Adkin, A.L., Quant, S., Maki, B.E., & McIlroy, W.E. (2006). Cortical responses associated with predictable and unpredictable compensatory balance reactions. *Experimental Brain Research, 172*, 85-93.

Ackermann, H., Dichgans, J., & Guschlbauer, B. (1991). Influence of an acoustic preparatory signal on postural reflexes of the distal leg muscles in humans. *Neuroscience Letters, 127*(2), 242-246.

Ackermann, H., Diener, H.C., & Dichgans, J. (1986). Mechanically evoked cerebral potentials and long-latency muscle responses in the evaluation of afferent and efferent long-loop pathways in humans. *Neuroscience Letters, 66*, 233-238.

Badgaiyan, R.D., & Posner, M.I. (1998). Mapping the cingulate cortex in response selection and monitoring. *Neuroimage, 7*, 255-260.

Beloozerova, I.N., Sirota, M.G., Orlovsky, G.N., & Deliagina, T.G. (2005). Activity of pyramidal tract neurons in the cat during postural corrections. *Journal of Neurophysiology, 93*, 1831–1844.

Beloozerova, I.N., Sirota, M.G., Swadlow, H.A., Orlovsky, G.N., Popova, L.B., & Deliagina, T.G. (2003). Activity of different classes of neurons of the motor cortex during postural corrections. *Journal of Neuroscience, 23*, 7844-7853.

Berger, W., Horstmann, G.A., & Dietz, V. (1990). Interlimb coordination of stance in children: Divergent modulation of spinal reflex responses and cerebral evoked potentials in terms of age. *Neuroscience Letters, 116*(1-2), 118-122.

Bernstein, P.S., Scheffers, M.K., & Coles, M.G.H. (1995). "Where did I go wrong?" A psychophysiological analysis of error detection. *Journal of Experimental Psychology: Human Perception and Performance, 21*, 1312-1322.

Blanke, O., Perrig, S., Thut, G., Landis, T., & Seeck, M. (2000). Simple and complex vestibular responses induced by electrical cortical stimulation of the parietal cortex in humans. *Journal of Neurology, Neurosurgery & Psychiatry, 69*(4), 553-556.

Brandt, T., Dieterich, M., & Danek, A. (1994). Vestibular cortex lesions affect the perception of verticality. *Annals of Neurology, 35*(4), 403-412.

Burleigh, A., & Horak, F. (1996). Influence of instruction, prediction, and afferent sensory information on the postural organization of step initiation. *Journal of Neurophysiology, 75*(4), 1619-1628.

Camilleri, J.M., Sibley, K.M., Zabjek, K.F., & McIlroy, W.E. (2006). *Investigating the role of the cortex following unexpected whole body perturbations.* Poster presented at Neuroscience 2006, Atlanta, GA. Abstract retrieved from http://www.abstractsonline.com/viewer/?mkey=%7BD1974E76-28AF-4C1C-8AE8-4F73B56247A7%7D

Carter, C.S., Braver, T.S., Barch, D.M., Botvinick, M.M., Noll, D., & Cohen, J.D. (1998). Anterior cingulate cortex, error detection, and the online monitoring of performance. *Science, 280*, 747-749.

Carter, C. S., MacDonald, A. W., III, Ross, L. L., & Stenger, V. A. (2001). Anterior cingulate cortex activity and impaired self-monitoring of performance in patients with schizophrenia: An event-related fMRI study. *American Journal of Psychiatry, 158*(9), 1423-1428.

Chan, C.W.Y., Melvill Jones, G., Kearney, R.E., & Watt, D.G.D. (1979). The 'late' electromyographic response to limb displacement in man. I. Evidence for supraspinal contribution. *Electroencephalography and Clinical Neurophysiology, 46*(2), 173-181.

Coles, M.G.H., Scheffers, M.K., & Holroyd, C. (1998). Berger's dream? The error-related negativity and modern cognitive psychophysiology. In Witte, H., Zwiener, U., Schjack, B., Döring, A. (Eds.). Quantitative and Topological EEG and MEG Analysis. Druckhaus Mayer Verlag, Jena-Erlangen, 96–102.

Coles, M.G.H., Scheffers, M.K., & Holroyd, C. (2000). Why is there an ERN or Ne on correct trials? *Psychophysiology, 37*(Suppl.1), S9.

Compumedics Neuroscan. (2007). *CURRY User Manual: Multi-modal Neuroimaging for CURRY 6*. El Paso, TX: Author.

Cuffin, B.N., Schomer, D.L., Ives, J.R., & Blume, H. (2001). Experimental tests of EEG source localization accuracy in realistically shaped head models. *Clinical Neurophysiology, 112*(12), 2288-2292.

de Waele, C., Baudonnière, P.M., Lepecq, J.C., Tran Ba Huy, P., & Vidal, P.P. (2001). Vestibular projections in the human cortex. *Experimental Brain Research, 141*, 541–551.

Dehaene, S., Posner, M.I., & Tucker, D.M. (1994). Localization of a neural system for error detection and compensation. *Psychological Science, 5*(5), 303-305.

Deliagina, T.G., Beloozerova, I.N., Zelenin, P.V., & Orlovsky, G.N. (2008). Spinal and supraspinal postural networks. *Brain Research Reviews, 57*, 212-221.

Dietz, V., Quintern, J., & Berger, W. (1984). Cerebral evoked potentials associated with the compensatory reactions following stance and gait perturbations. *Neuroscience Letters, 50*, 181-186.

Dietz, V., Quintern, J., & Berger, W. (1985). Afferent control of human stance and gait: Evidence for blocking group I afferents during gait. *Experimental Brain Research, 61*, 153-163.

Dietz, V., Quintern, J., Berger, W., & Schenck, E. (1985). Cerebral potentials and leg muscle e.m.g. responses associated with stance perturbation. *Experimental Brain Research, 57*, 348-354.

Dimitrov, B., Gavrilenko, T., & Gatev, P. (1996). Mechanically evoked cerebral potentials to sudden ankle dorsiflexion in human subjects during standing. *Neuroscience Letters, 208*, 199-202.

Duckrow, R.B., Abu-Hasaballah, K., Whipple, R., & Wolfson, L. (1999). Stance perturbation-evoked potentials in old people with poor gait and balance. *Clinical Neurophysiology, 110*, 2026-2032.

Falkenstein, M., Hohnsbein, J., Hoormann, J., & Blanke, L. (1990). Effects of errors in choice reaction tasks on the ERP under focused and divided attention. In *Psychophysiological Brain Research* (C.H.M. Brunia, A.W.K. Gaillard, & A. Kok, Eds.), 192-195. Tilburg University Press, Tilburg, The Netherlands.

Falkenstein, M., Hohnsbein, J., Hoormann, J., & Blanke, L. (1991). Effects of crossmodal divided attention on late ERP components. II. Error processing in choice reaction time tasks. *Electroencephalography and Clinical Neurophysiology, 78*, 447-455.

Falkenstein, M., Hoormann, J., Christ, S., & Hohnsbein, J. (2000). ERP components on reaction errors and their functional significance: A tutorial. *Biological Psychology, 51*, 87-107.

Falkenstein, M., Koshlykova, N.A., Kiroj, V.N., Hoormann, J., & Hohnsbein, J. (1995). Late ERP components in visual and auditory Go/Nogo tasks. *Electroencephalography and Clinical Neurophysiology, 96*, 36-43.

Fiehler, K., Ullsperger, M., & von Cramon, D.Y. (2005). Electrophysiological correlates of error correction. *Psychophysiology, 42*, 72-82.

Gage, W.H., Zabjek, K.F., Hill, S.W., & McIlroy, W.E. (2007). Parallels in control of voluntary and perturbation-evoked reach-to-grasp movements: EMG and kinematics. *Experimental Brain Research, 181*(4), 627-637.

Gehring, W.J. (1992). The error-related negativity: Evidence for a neural mechanism for error-related processing. Doctoral dissertation, University of Illinois at Urbana-Champaign.

Gehring, W.J., Coles, M.G.H., Meyer, D.E., & Donchin, E. (1990). The error-related negativity: An event-related brain potential accompanying errors. *Psychophysiology, 27*, 34.

Gehring, W.J., Goss, B., Coles, M.G.H., Meyer, D.E., & Donchin, E. (1993). A neural system for error detection and compensation. *Psychological Science, 4*(6), 385-390.

Gemba, H., & Sasaki, K. (1989). Potential related to no-go hand movement task with color discrimination in humans. *Neuroscience Letters, 101*, 263-268.

Gemba, H., Sasaki, K., & Brooks, V.B. (1986). 'Error' potentials in limbic cortex (anterior cingulate area 24) of monkeys during motor learning. *Neuroscience Letters, 70*, 223–227.

Ghafouri, M., McIlroy, W.E., & Maki, B.E. (2004). Initiation of rapid reach-and-grasp balance reactions: is a pre-formed visuospatial map used in controlling the initial arm trajectory? *Experimental Brain Research, 155*(4), 532-536.

Hanakawa, T., Fukuyama, H., Katsumi, Y., Honda, M., & Shibasaki, H. (1999). Enhanced lateral premotor activity during paradoxical gait in Parkinson's disease. Annals of Neurology, 45(3), 329-336.

Hodges, P.W., & Bui, B.H. (1996). A comparison of computer-based methods for the determination of onset of muscle contraction using electromyography. *Electroencephalography and Clinical Neurophysiology, 101*(6), 511-519.

Holroyd, C.B., & Coles, M.G.H. (2002). The neural basis of human error processing: Reinforcement learning, dopamine, and the error-related negativity. *Psychological Review, 109*(4), 679-709.

Holroyd, C.B., Dien, J., & Coles, M.G.H. (1998). Error-related scalp potentials elicited by hand and foot movements: Evidence for an output-independent error-processing system in humans. *Neuroscience Letters, 242*, 65-68.

Holroyd, C.B., Nieuwenhuis, S., Yeung, N., Nystrom, L., Mars, R., Coles, M.G.H., et al. (2004). Dorsal anterior cingulate cortex shows fMRI response to internal and external error signals. *Nature Neuroscience, 7*(5), 497-498.

Honeycutt, C.F., & Nichols, T.R. (2006). *Force responses of the postural strategy in the decerabrate cat.* Poster presented at Neuroscience 2006, Atlanta, GA. Abstract retrieved from http://www.abstractsonline.com/viewer/?mkey=%7BD1974E76-28AF-4C1C-8AE8-4F73B56247A7%7D

Horak, F.B., & Nashner, L.M. (1986). Central programming of postural movements: Adaptation to altered support-surface configurations. *Journal of Neurophysiology, 55*(6), 1369-1381.

Jacobs, J.V., Fujiwara, K., Tomita, H., Furune, N., Kunita, K., & Horak, F.B. (2008). Changes in the activity of the cerebral cortex relate to postural response modification when warned of a perturbation. *Clinical Neurophysiology, 119*(6), 1431-1442.

Jacobs, J.V., & Horak, F.B. (2006). Abnormal proprioceptive-motor integration contributes to hypometric postural responses of subjects with Parkinson's disease. *Neuroscience, 141*(2), 999-1009.

Jacobs, J.V. & Horak, F.B. (2007). Cortical control of postural responses. *Journal of Neural Transmission, 114*, 1339-1348.

Jobges, M., Heuschkel, G., Pretzel, C., Illhardt, C., Renner, C., & Hummelsheim, H. (2004). Repetitive training of compensatory steps: a therapeutic approach for postural instability in Parkinson's disease. *Journal of Neurology, Neurosurgery and Psychiatry, 75*(12), 1682-1687.

Johannsen, L., Broetz, D., Naegele, T., & Karnath, H.O. (2006). "Pusher syndrome" following cortical lesions that spare the thalamus. *Journal of Neurology, 253*(4), 455-463.

Karayannidou, A., Tamarova, Z.A., Sirota, M.S., Zelenin, P.V., Orlovsky, G.N., Deliagina, T.G., et al. (2006). Integration of sensory inputs from different limbs in postural responses of pyramidal tract neurons. Poster presented at Neuroscience 2006, Atlanta, GA. Abstract retrieved from http://www.abstractsonline.com/viewer/viewAbstract.asp?CKey={8F1AAA4D-ACA8-4D84-A0BC-99E2CFB49A9A}&MKey={D1974E76-28AF-4C1C-8AE8-4F73B56247A7}&AKey={3A7DC0B9-D787-44AA-BD08-FA7BB2FE9004}&SKey={C3ED3905-4CAF-4873-BC28-366C668B5888}

Kerns, J.G., Cohen, J.D., MacDonald, A.W., Cho, R.Y., Stenger, V.A., & Carter, C.S. (2004). Anterior cingulate conflict monitoring and adjustments in control. *Science, 303*, 1023-1026.

Kiefer, M., Marzinzik, F., Weisbrod, M., Scherg, M., & Spitzer, M. (1998). The time course of brain activations during response inhibition: Evidence from event-related potentials in a go/no go task. *NeuroReport, 9*, 765-770.

Kiehl, K.A., Liddle, P.F., & Hopfinger, J.B. (2000). Error processing and the rostral anterior cingulate: An event-related fMRI study. *Psychophysiology, 37*, 216-223.

Maeda, K., & Fujiwara, K. (2007). Effects of preparatory period on anticipatory postural control and contingent negative variation associated with rapid arm movement in standing posture. *Gait & Posture, 25*(1), 78-85.

Maki, B.E., & McIlroy, W.E. (2007). Cognitive demands and cortical control of human balance-recovery reactions. *Journal of Neural Transmission, 114*, 1279–1296.

Martin, J.H. (2003). *Neuroanatomy: Text and Altas.* (3rd ed.). Columbus (OH): McGraw-Hill Companies, Inc.

Matsuyama, K., & Drew, T. (2000). Vestibulospinal and reticulospinal neuronal activity during locomotion in the intact cat. II. Walking on an inclined plane. *Journal of Neurophysiology. 84*, 2257–2276.

Maurer, C., Mergner, T., Bolha, B., & Hlavacka, F. (2000). Vestibular, visual, and somatosensory contributions to human control of upright stance. *Neuroscience Letters, 281*, 99-102.

McIlroy, W.E., & Maki, B.E., (1997). Preferred placement of the feet during quiet stance: Development of a standardized foot placement for balance testing. *Clinical Biomechanics, 12*(1), 66-70.

McIlroy, W.E., Norrie, R.G., Brooke, J.D., Bishop, D.C., Nelson, A.J., & Maki, B.E. (1999). Temporal properties of attention sharing consequent to disturbed balance. *NeuroReport, 10*, 2895–2899.

Menon, V., Adleman, N.E., White, C.D., Glover, G.H., & Reiss, A.L. (2001). Error-related brain activation during a Go/NoGo response inhibition task. *Human Brain Mapping, 12*, 131-143.

Mergner, T., Maurer, C., & Peterka, R.J. (2003). A multisensory posture control model of human upright stance. *Progress in Brain Research, 142*, 189-201.

Miltner, W.H.R., Braun, C.H., & Coles, M.G.H. (1997). Event-related brain potentials following incorrect feedback in a time-estimation task: Evidence for a "generic" neural system for error detection. *Journal of Cognitive Neuroscience, 9*(6), 788- 798.

Miltner, W.H.R., Lemke, U., Holroyd, C., Scheffers, M.K., & Coles, M.G.H. (1998). Where does the brain process errors? On the neural generators of the ERN. *Psychophysiology, 35*(Suppl. 1), S7.

Miltner, W.H.R., Lemke, U., Weiss, T., Holroyd, C., Scheffers, M.K., & Coles, M.G.H. (2003). Implementation of error-processing in the human anterior cingulate cortex: A source analysis of the magnetic equivalent of the error-related negativity. *Biological Psychology, 64*, 157-166.

Mochizuki, G., Boe, S., Marlin, A., & McIlroy, W.E. (2010). Perturbation-evoked cortical activity reflects both the context and consequence of postural instability. *Neuroscience, 170*(2), 599-609.

Mochizuki, G., Sibley, K.M., Cheung, H.J., Camilleri, J.M., & McIlroy, W.E. (2009). Generalizability of perturbation-evoked cortical potentials: Independence from sensory, motor and overall postural state. *Neuroscience Letters, 451*(1), 40-44.

Mochizuki, G., Sibley, K.M., Cheung, H.J., & McIlroy, W.E. (2009). Cortical activity prior to predictable postural instability: Is there a difference between self-initiated and externally initiated perturbations? *Brain Research, 1279*, 29-36.

Mochizuki, G., Sibley, K.M., Esposito, J.G., Camilleri, J.M., & McIlroy, W.E. (2007). *Predictability of perturbations to standing balance influence the characteristics of early and late cortical potentials.* Poster presented at Neuroscience 2007, San Diego, CA. Abstract retrieved from http://www.abstractsonline.com/viewer/?mkey=%7BFF8B70E5-B7F9-4D07-A58A-C1068FDE9D25%7D

Mochizuki, G., Sibley, K.M., Esposito, J.G., Camilleri, J.M., & McIlroy, W.E. (2008). Cortical responses associated with the preparation and reaction to full-body perturbations to upright stability. *Clinical Neurophysiology, 119*, 1626-1637.

Mochizuki, G., Zabukovec, J., Sibley, K.M., & McIlroy, W.E. (2009). *Generalizability of perturbation-evoked cortical potentials: Cortical activity linked to temporally-urgent responses.* Poster presented at the 19th International Conference of the International Society for Posture & Gait Research (ISPGR), Bologna, Italy. Abstract retrieved from http://ispgr.org/fileadmin/templates/_docs/2009/italy2009-presenters.pdf

Nashner, L. (1976). Adapting reflexes controlling the human posture. *Experimental Brain Research, 26*(1), 59-72.

Niki, H., & Watanabe, M. (1979). Prefrontal and cingulate unit activity during timing behavior in the monkey. *Brain Research, 171*, 213-224.

Norrie, R.G., Maki, B.E., Staines, W.R., & McIlroy, W.E. (2002). The time course of attention shifts following perturbation of upright stance. *Experimental Brain Research, 146*, 315–321.

Ouchi, Y., Okada, H., Yoshikawa, E., Nobezawa, S., & Futatsubashi, M. (1999). Brain activation during maintenance of standing postures in humans. *Brain, 122*(Part 2), 329-338.

Pailing, P.E., & Segalowitz, S.J. (2004). The effects of uncertainty in error monitoring on associated ERPs. *Brain and Cognition, 56*, 215-233.

Perennou, D.A., Leblond, C., Amblard, B., Micallef, J.P., Rouget, E., & Pelissier, J. (2000). The polymodal sensory cortex is crucial for controlling lateral postural stability: Evidence from stroke patients. *Brain Research Bulletin, 53*(3), 359-365.

Quant, S., Adkin, A.L., Staines, W.R., Maki, B.E., & McIlroy, W.E. (2004). The effect of a concurrent cognitive task on cortical potentials evoked by unpredictable balance perturbations. *BMC Neuroscience, 5*, 18.

Quant, S., Adkin, A.L., Staines, W.R., & McIlroy, W.E. (2004). Cortical activation following a balance disturbance. *Experimental Brain Research, 155*, 393-400.

Quintern, J., Berger, W., & Dietz, V. (1985). Compensatory reactions to gait perturbations in man: Short- and long-term effects of neuronal adaptation. *Neuroscience Letters, 62*, 371-376.

Rankin, J.K., Woollacott, M.H., Shumway-Cook, E., & Brown, L.A. (2000). Cognitive influence on postural stability: A neuromuscular analysis in young and older adults. *Journals of Gerontology Series A: Biological Sciences and Medical Sciences, 55*, M112-M119.

Rapport, L.J., Webster, J.S., Flemming, K.L., Lindberg, J.W., Godlewski, M.C., Brees, J.E., et al. (1993). Predictors of falls among right-hemisphere stroke patients in the rehabilitation setting. *Archives of Physical Medicine and Rehabilitation, 74*, 621-626.

Roberts, L.E., Rau, H., Lutzenberger, W., & Birbaumer, N. (1994). Mapping P300 waves onto inhibition: Go/No-Go discrimination. *Electroencephalography and Clinical Neurophysiology, 92*, 44-55.

Rogers, M.W., Johnson, M.E., Martinez, K.M., Mille, M.L., & Hedman, L.D. (2003). Step training improves the speed of voluntary step initiation in aging. *Journals of Gerontology Series A: Biological Sciences and Medical Sciences, 58*(1), 46-51.

Sasaki, K., & Gemba, H. (1986). Electrical activity in the prefrontal cortex specific to no-go reaction of conditioned hand movement with colour discrimination in the monkey. *Experimental Brain Research, 64*, 603-606.

Scheffers, M.K., & Coles, M.G.H. (2000). Performance monitoring in a confusing world: Error-related brain activity, judgments of response accuracy, and types of errors. *Journal of Experimental Psychology: Human Perception and Performance, 26*(1), 141-151.

Scheffers, M.K., Coles, M.G.H., Bernstein, P., Gehring, W.J., & Donchin, E. (1996). Event-related brain potentials and error-related processing: An analysis of incorrect responses to go and no-go stimuli. *Psychophysiology, 33*, 42-53.

Shima, K., & Tanji, J. (1998). Role for cingulate motor area cells in voluntary movement selection based on reward. *Science, 282*, 1335-1338.

Sibley, K.M., Lakhani, B., Mochizuki, G., & McIlroy, W.E. (2010). Perturbation-evoked electrodermal responses are sensitive to stimulus and context-dependent manipulations of task challenge. *Neuroscience Letters, 485*(3), 217-221.

Slobounov, S., Wu, T., & Hallett, M. (2006). Neural basis subserving the detection of postural instability: An fMRI study. *Motor Control, 10*, 69-89.

Staines, W.R., McIlroy, W.E., & Brooke, J.D. (2001). Cortical representation of whole-body movement is modulated by proprioceptive discharge in humans. *Experimental Brain Research, 138*, 235-242.

Taube, W., Schubert, M., Gruber, M., Beck, S., Faist, M., & Gollhofer, A. (2006). Direct corticospinal pathways contribute to neuromuscular control of perturbed stance. *Journal of Applied Physiology, 101*, 420-429.

Teasdale, N. & Simoneau, M. (2001). Attentional demands for postural control: The effects of aging and sensory reintegration. *Gait & Posture, 14*, 203-210.

Tripp, B.P., McIlroy, W.E., & Maki, B.E. (2004). Online mutability of step direction during rapid stepping reactions evoked by postural perturbation. *IEEE Transactions on Neural Systems and Rehabilitation Engineering, 12*(1), 140-152.

Ullsperger, M., & von Cramon, D.Y. (2001). Subprocesses of performance monitoring: A dissociation of error processing and response competition revealed by event-related fMRI and ERPs. *NeuroImage, 14*, 1387-1401.

Ullsperger, M., & von Cramon, D.Y. (2003). Error monitoring using external feedback: Specific roles of the habenular complex, the reward system, and the cingulate motor area revealed by functional magnetic resonance imaging. *Journal of Neuroscience, 23*(10), 4308-4314.

van Veen, V., & Carter, C.S. (2002a). The anterior cingulate as a conflict monitor: fMRI and ERP studies. *Physiology & Behavior, 77*, 477-482.

van Veen, V., & Carter, C.S. (2002b). The timing of action-monitoring processes in the anterior cingulate cortex. *Journal of Cognitive Neuroscience, 14*(4), 593-602.

Yasuda, A., Sato, A., Miyawaki, K., Kumano, H., & Kuboki, T. (2004). Error-related negativity reflects detection of negative reward prediction error. *NeuroReport, 15*, 2561-2565.

Yeung, N., Botvinick, M.M., & Cohen, J.D. (2004). The neural basis of error detection: Conflict monitoring and the error-related negativity. *Psychological Review, 111*(4), 931-959.

Yoshida, S., Nakazawa, K., Shimizu, E., & Shimoyama, I. (2008). Anticipatory postural adjustments modify the movement-related potentials of upper extremity voluntary movement. *Gait & Posture, 27*(1), 97-102.

Zettel, J.L., Holbeche, A., McIlroy, W.E., & Maki, B.E. (2005). Redirection of gaze and switching of attention during rapid stepping reactions evoked by unpredictable postural perturbation. *Experimental Brain Research, 165*(3), 392-401.

Zettel, J.L., McIlroy, W.E., & Maki, B.E. (2002a). Can stabilizing features of rapid triggered stepping reactions be modulated to meet environmental constraints? *Experimental Brain Research, 145*(3), 297-308.

Zettel, J.L., McIlroy, W.E., & Maki, B.E. (2002b). Environmental constraints on foot trajectory reveal the capacity for modulation of anticipatory postural adjustments during rapid triggered stepping reactions. *Experimental Brain Research, 146*(1), 38-47.